

Dr
M.A.T
1399

Thermo-Solutal Nanofluid Flow by Exponential Stretching Sheet with Thermal Radiation



By

Madiha Rashid

**Department of Mathematics
Quaid-i-Azam University
Islamabad, Pakistan
2015**

Thermo-Solutal Nanofluid Flow by Exponential Stretching Sheet with Thermal Radiation



By

Madiha Rashid

Supervised By

Dr. Muhammad Ayub

Department of Mathematics
Quaid-i-Azam University
Islamabad, Pakistan
2015

Thermo-Solutal Nanofluid Flow by Exponential Stretching Sheet with Thermal Radiation



By
Madiha Rashid

A DISSERTATION SUBMITTED IN THE PARTIAL FULFILLMENT OF THE
REQUIREMENTS FOR THE DEGREE OF THE MASTER OF PHILOSOPHY

IN

MATHEMATICS

Supervised By

Prof. Dr. Muhammad Ayub

Department of Mathematics
Quaid-i-Azam University
Islamabad, Pakistan
2015

Thermo-Solutal Nanofluid Flow by Exponential Stretching Sheet with Thermal Radiation

By

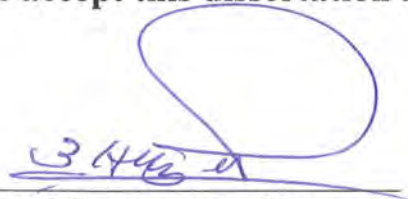
Madiha Rashid

CERTIFICATE

**A DISSERTATION SUBMITTED IN THE PARTIAL FULFILLMENT OF THE
REQUIREMENTS FOR THE DEGREE OF THE MASTER OF PHILOSOPHY**

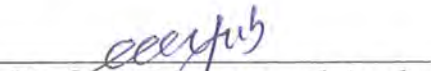
We accept this dissertation as conforming to the required standard

1.



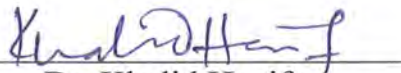
Prof. Dr. Tasawar Hayat
(Chairman)

2.



Prof. Dr. Muhammad Ayub
(Supervisor)

3.



Dr. Khalid Hanif
(External Examiner)

**Department of Mathematics
Quaid-i-Azam University
Islamabad, Pakistan
2015**

Dedicated
to my beloved Father
who left me for their eternal abode
during my M.Phil,
but I always feel their prayers with me,
to my Mother who provided me the
support and encouragement.

ACKNOWLEDGEMENTS

I am start my acknowledgement with the highest gratitude to Almighty ALLAH, who bestowed me with His uncountable blessings which enabled me to coup with this challenging and strenuous task. In truth, the path to the love of Allah is bound with the love of His Messenger. The Prophet (PBUH) himself relates in one of his sayings how the love for him is interrelated with faith.

It would not have been possible to write this thesis without the help and support of kind people around me. However, only some of them can be particularly mentioned here.

I would like to express my deepest gratitude to my supervisor, Prof. Dr. Muhammad Ayub and co-supervisor Prof. Dr. Tasawar Hayat. Their abundant patience, valuable contribution, guidance and perpetual encouragement has helped me in my research work.

I am keenly indebted to Maria Imtiaz for his constant support, precious indications and patience. I cannot begin to describe how my understanding of mathematics has grown under her watch. I have learned extensively and grateful for the knowledge

and experience she have shared with me in many conversations.

Firstly, I convey my special tribute to my father (late), whose unseen presence is always a source of strength and inspiration for me. Lastly, I am very thankful to my mother for her guidance and support. Her love, compassion, encouragement, and desire to see me succeed at every turn of this winding path were immeasurable. I owe my heartiest gratitude for her assistance and never ending prayers for my success. I highly commend the cooperative behavior of my brothers who endeavored for my edification and betterment.

I am grateful to Muhammad Farooq for their valuable discussion in my M.Phil. Research work. I am also thankful to my friends especially Eman Shahid and Wajeeha Shinwari for extending valuable moral support and dedicated guidance whenever required. Their company really made my time beautiful and full of joys with everlasting memories.

Madiha Rashid

June 22, 2015

Preface

Nanofluid is hot topic of research during the last few years. "Nanofluids" are relatively new class of fluids which consists of a base fluid with suspended nano-sized metallic or non-metallic particles (1–100 nm). The nanoparticles used in nanofluids are typically made of metals, oxides, carbides, or carbon nanotubes. These nanoparticles have been found to possess enhanced thermophysical properties such as thermal conductivity, thermal diffusivity and convective heat transfer coefficients when compared to those of base fluids. Choi [1] worked firstly about the analysis of nanoparticles. He experimentally found that addition of nanoparticles in conventional/base fluid remarkably enhances the thermal conductivity of the base fluid. Buongiorno [2] developed a model for convective transport in nanofluids by considering Brownian diffusion and thermophoresis effects. It is now known that novel properties of nanofluids make them potentially useful in many applications such as polymer industry, paper production, food processing, crystal growing, microelectronics, fuel cells, pharmaceutical and hybrid power engines, engine cooling/vehicle thermal management, domestic refrigerator, chiller heat exchanger in grinding, boiler flue gas temperature reduction and many others. Especially the magnetic nanoparticles have important applications in medicine and engineering. Many equipment's such as MHD generators, pumps, bearings and boundary layer control are affected by the interaction between the electrically conducting fluid and a magnetic field. Numerous applications involving magneto nanofluids include drug delivery, hyperthermia, contrast enhancement in magnetic resonance imaging and magnetic cell separation. Motivated by all the aforementioned facts, various scientists and engineers are engaged in the discussion of flows of nanofluids via different aspects (see [3–12] and many useful attempts therein).

The fluid flow over stretching surface has gained the attention of researchers due to its important applications in engineering processes namely polymer extrusion, drawing of plastic films and wires, glass fiber and paper production, manufacture of foods, crystal growing, liquid films in condensation process, etc. Crane [13] deals with the study of boundary layer flow over stretching surface where the velocity of the stretching surface is assumed linearly proportional to the distance from the fixed origin. However, it has often been argued that, realistically, the stretching of a sheet might be nonlinear. Flow and heat transfer characteristics past an exponentially stretching sheet has a wider applications in technology. For example, in case of annealing and thinning of copper wires, the final product depends on the rate of heat transfer at the surface with exponential variations of stretching velocity. During such processes, both the kinematics of stretching and the simultaneous heating or cooling have a decisive influence on the quality of the final product. Specific example in this direction can be mentioned through process in plastic industry. This situation was tackled by Mukhopadhyay [14] who has been investigated the slip effects on MHD boundary layer flow by an exponentially stretching sheet with suction/blowing and thermal radiation. Exact solutions for two-dimensional laminar flow over a continuously stretching or shrinking sheet in an electrically conducting quiescent couple stress fluid have been derived by Turkyilmazoglu [15]. Ibrahim et al. [16] analyzed the MHD stagnation point flow of nanofluid towards a stretching sheet. Slip effects on unsteady stagnation point flow of nanofluid over a stretching sheet are investigated by Malvandi et al. [17]. Hayat et al. [18] examined the MHD flow of nanofluids by an exponentially stretching sheet with convective boundary conditions. Stratification of fluid arises not only for temperature variation but also for the

concentration differences. The effect of stratification is an important aspect in heat and mass transfer and it has been studied by several researchers. This phenomenon occurs due to the change in temperature or concentration, or variations in both, or presence of fluids with different densities. Density differences in the presence of gravity have a key role on the dynamics and mixing of heterogeneous fluid. Examples include thermal stratification of reservoirs and oceans, salinity stratification in estuaries, rivers, groundwater reservoirs and oceans, heterogeneous mixtures in industrial, food and manufacturing processing, density stratification of the atmosphere and uncountable similar examples. In the presence of gravity, these density differences have a dramatic impact on the dynamics and mixing of heterogeneous fluids. For example thermal stratification in reservoirs can reduce the mixing of oxygen to the bottom water to become anoxic through the action of biological processes. Stratification plays important role in lakes and ponds since it controls the temperature and concentration differences of hydrogen and oxygen in such environments which may affect the growth rate of various species. Also the analysis of thermal stratification is important for solar engineering because higher energy efficiency can be achieved with better stratification. Mukhopadhyay [20] reported MHD flow of viscous fluid induced by an exponentially stretching sheet in thermally stratified medium. Srinivasacharya and Upendar [21] examined MHD free convection flow of micropolar fluid with double stratification. Hayat et al. [22] examined the thermal stratification effects in mixed convective flow of Maxwell fluid over a stretching surface. Thermally stratified stagnation point flow of an Oldroyd-B fluid is discussed by Hayat et al. [23].

This dissertation is arranged as follows:

Chapter one contains some standard definitions and fundamental equations useful for flow analysis of subsequent chapters.

Chapter two presents the problem of boundary layer viscous two dimensional nanofluid flow induced by a stretchable surface. Homotopy analysis method (HAM) is carried out to solve the above phenomena. Numerical values of heat and mass transfer coefficients are presented in tabular form. This chapter is a detailed review of a paper by Hassani et.al [24].

Chapter three constitutes the analytical solution for steady boundary layer flow of nanofluid past an exponential stretchable surface. Heat and mass transfer phenomenon is examined under the influence of double stratified medium. Effects of porous medium and thermal radiation are also encountered. Homotopy analysis method (HAM) [25-30] is utilized to solve the arising mathematical problem. Through graphical illustrations, impact of pertinent parameters are investigated.

Contents

1	Elementary concepts and standard definitions	4
1.0.1	Fluid	4
1.0.2	Fluid mechanics	4
1.0.3	Density	4
1.0.4	Viscosity	5
1.1	Types of flow	5
1.1.1	Steady vs unsteady flow	5
1.1.2	Compressible vs incompressible flow	5
1.2	Classification of fluids	5
1.2.1	Inviscid and viscous fluids	5
1.2.2	Newtonian fluids	6
1.2.3	Non-Newtonian fluids	6
1.3	Nanofluid	7
1.3.1	Buongiorno's model	7
1.3.2	Phase flow model	7
1.4	Boundary layer approximation	8
1.5	Thermal conductivity	8
1.6	Enthalpy	9
1.7	Specific heat	9
1.8	Porous medium	9
1.9	Magnetohydrodynamics	10
1.10	Viscous dissipation	11

1.11 Stratification	11
1.11.1 Thermal stratification	12
1.11.2 Sloutal stratification	12
1.12 Physical description of dimensionless numbers	12
1.12.1 Reynolds number	12
1.12.2 Brownian motion parameter	13
1.12.3 Thermophoresis parameter	13
1.12.4 Schmidt number	13
1.12.5 Prandtl number	14
1.12.6 Eckert number	14
1.12.7 Hartman number	14
1.12.8 Nusselt number	15
1.12.9 Sherwood number	15
1.12.10 Skin friction coefficient	15
1.13 Constitutive equation	16
1.13.1 Conservation of mass	16
1.13.2 Conservation of linear momentum	16
1.13.3 Conservation of energy	17
1.13.4 Conservation of concentration	19
1.14 Solution methodology	19
1.14.1 Homotopy analysis method	20
2 Boundary layer nanofluid flow past a stretching sheet	21
2.1 Mathematical formulation	22
2.2 Homotopy solution	24
2.2.1 Zeroth order deformation equations	24
2.2.2 Deformation problems of mth-order	26
2.3 Convergence of HAM solution	26
2.4 Results and discussion	28
2.5 Key findings	32

3	MHD effects on thermo-solutal stratified nanofluid flow by an exponential stretching sheet with thermal radiation	33
3.1	Problem formulation	34
3.2	Homotopy solution	37
3.2.1	Zeroth order deformation equations	37
3.2.2	mth-order deformation problems	39
3.3	Convergence of HAM solution	40
3.4	Graphical results and discussion	42
3.5	Key findings	51



Chapter 1

Elementary concepts and standard definitions

In this chapter, we include some standard definitions and fundamental equations useful for flow analysis of subsequent chapters. Also we discussed solution methodology i.e. homotopy analysis method.

1.0.1 Fluid

Fluid is the material that flows and continuously deforms under an applied shear stress.

1.0.2 Fluid mechanics

It is the branch of engineering that examines the nature and properties of fluids, both in motion and at rest.

1.0.3 Density

The mass per unit volume at a given temperature and pressure or stress condition is expressed by equation

$$\rho = \lim_{\delta V \rightarrow 0} \frac{\delta M}{\delta V}, \quad (1.1)$$

where δM is the mass of fluid and δV is the volume element.

1.0.4 Viscosity

Viscosity is a physical property of fluids associated with shearing deformation of fluid particles subjected to the action of any applied force.

1.1 Types of flow

There are many types of flow, among of these following are important from the subject point of view:

1.1.1 Steady vs unsteady flow

In steady flow the quantity of liquid flowing per second is constant. A steady flow may be uniform or non-uniform while in unsteady flow the quantity of liquid flowing per second is not constant.

1.1.2 Compressible vs incompressible flow

A compressible flow contains the volume and thus the density of the flowing liquid changes during the flow (i.e. gases) while incompressible flow contains the volume and thus the density of the flowing liquid does not changes during the flow (i.e. liquids).

1.2 Classification of fluids

1.2.1 Inviscid and viscous fluids

Whenever the normal as well as shearing stresses exist, viscous fluids are occupied. This is due to the fact that the shearing stresses by a viscous fluid produce a resistance to the moving body (substances) across it as well as between the particles of the fluid itself. Instead of this when a fluid does not exert any shearing stress, inviscid fluid is occurred whether it is in the state of rest or in motion. Clearly the pressure exerted by an inviscid fluid on any surface is always along the normal to the surface at that point. Note that all natural fluids including the synthetic fluids are real fluids and exhibits viscosity effects. An inviscid fluid is a fictitious fluid and does not exist in nature. However many fluids under certain engineering applications show

negligible viscosity effects and can be treated as inviscid fluid. Air and water are inviscid fluids whereas syrup and heavy oil are treated as viscous fluids.

1.2.2 Newtonian fluids

Those fluids for which stress at each point possess a linear relationship between the shear stress and shear rate of fluids are known as Newtonian fluids. These fluids follow the Newton's law of viscosity. Mathematically

$$\tau_{yx} \propto \frac{du}{dy}, \quad (1.2)$$

$$\tau_{yx} = \mu \frac{du}{dy}, \quad (1.3)$$

here x -direction contains u component of velocity, du/dy the deformation rate, τ_{yx} the shear stress and μ the proportionality constant is known as dynamic viscosity. Also for Newtonian fluids the viscosity is independent of the rate of deformation. Sugar solution (glucose), water, glycerin, kerosene, thin motor and silicone oils are the relevant examples of Newtonian fluids.

1.2.3 Non-Newtonian fluids

For non-Newtonian fluids power-law model holds, i.e.

$$\tau_{yx} \propto \left(\frac{du}{dy} \right)^n, n \neq 1, \quad (1.4)$$

$$\tau_{yx} = k_a \left(\frac{du}{dy} \right)^n. \quad (1.5)$$

Eq. (1.4) become a Newton's law of viscosity for $n = 1$ with $k_a = \mu$. Here n is the flow behavior index and k_a is consistency index. Eq. (1.5) represents the power law model for one dimensional flow so we have

$$\tau_{yx} = \xi \left(\frac{du}{dy} \right), \quad (1.6)$$

where the apparent viscosity ξ is

$$\xi = k_a \left(\frac{du}{dy} \right)^{n-1}, n \neq 1. \quad (1.7)$$

We cannot take the negative values of n , because power law does not hold for negative values. In this case, shear stresses does not remain directly proportional. Soap, jelly, toothpaste, blood, ketchup, licite paint, drilling muds and biological fluids are relevant examples.

1.3 Nanofluid

Nanofluids are homogeneous mixture of base fluid and colloidal suspension of nanoparticles. Unlike heat transfer in conventional fluids, the exceptionally high thermal conductivity and enhanced heat transfer rates provide a unique feature of nanofluid. It is introduced by Choi on Argon National Laboratory at 1995. Thermal conductivity of the fluid can raise upto 20% comparatively by adding less volume fraction of nanoparticles (1 – 5%). The factors upon which such enhancement depends are the density, dimensions, shape, thermal ability of material and volume fraction of nanoparticles in the suspensions. The interest of researchers in nanofluid grows fast due to its several industrial, engineering and technological applications such as chemical catalytic reactors, grain storage installations, diffusion of medicine in blood veins and cooling of electronic apparatus.

1.3.1 Buongiorno's model

Buongiorno proposed a mathematical model to capture the nanoparticles/base fluid slip by treating nanofluid as two component mixture, base fluid and nanoparticles. Considered seven slip mechanisms and concluded that Brownian motion and thermophoresis are important slip mechanisms.

1.3.2 Phase flow model

In general, the nanofluids used for the purpose of enhanced heat transfer are dilute fluids and the volume fractions of nanoparticles are below 5 – 10%. Since the solid particles are ultra fine (less than 100nm) and they are easily fluidized, these particles (spherical shaped) can be approximately considered to behave like a fluid. Thermal properties involved in calculating the heat transfer rate of the nanofluid are viscosity, density, heat capacity and thermal conductivity. These properties are expressed in terms of nanoparticles volume fraction.

1.4 Boundary layer approximation

Most flow fields do not have exact solutions. But with the use of characteristics scale many valuable solutions are obtained for different physical problems. In this, terms having negligible contribution are neglected to give rise the approximate equations for the problem under consideration. Reynolds number takes small values in boundary layer specially near the bounding surface i.e. scale along bounding surface is L and length scale perpendicular to bounding surface is δ such that

$$\delta \ll L,$$

we have the basic assumption for the boundary layer approximation as follows:

Firstly, the velocity beyond the boundary layer is of the order U which is considered as free stream velocity. Secondly, by characteristic length L which is independent of v , x -direction containing the derivatives can be estimated. Thirdly, due to this length scale the thickness of the boundary layer has a characteristic size δ having condition $\delta \ll L$ derivatives in y -direction. Lastly the external influence is absent (like e.g. a shock wave) and provides a special scale for the pressure gradient which adapts the other terms in the equations. We know that boundary layers are thin so we expect

$$\frac{\delta}{L} \ll 1, \quad (1.8)$$

where $\frac{\delta}{L}$ always work in non-dimensional term and 1 is the order of magnitude.

1.5 Thermal conductivity

It is the characteristic of any substance which has ability to conduct heat. It is defined as the amount of heat Q_r transmitted through some thickness (b) per unit time (t) held perpendicularly to a surface area (A) which is caused by temperature difference ($T_u - T_l$). Mathematically, it can be expressed by

$$k = \frac{Q_r b}{t A (T_u - T_l)}, \quad (1.9)$$

where T_u and T_l are the temperatures measured along the thickness b . This definition is followed by the "Fourier law of heat conduction". This law gives a vector relationship between



rate of heat transfer and temperature gradient. Thermal conductivity depends on temperature, density, phase of the medium and molecular bonding.

1.6 Enthalpy

A thermodynamical quantity which is equal to the internal energy of a system plus the product of its volume and pressure. It is denoted by the symbol H and is defined as

$$H = A + p\tilde{V}. \quad (1.10)$$

Here A is the internal energy, p is the pressure and \tilde{V} is the volume of the system. At any given time the value of enthalpy is determined by the temperature, composition of the system and pressure.

1.7 Specific heat

Amount of energy which is transferred to or from mole of a any substance to provide a change in its temperature by one degree is known as specific heat. It is an extensive property which depends on the substance under consideration. The state of specific heat is specified by its properties. It is denoted by the symbol C_p . The equation in which the mass is the unit quantity and the heat energy is relative to the specific heat capacity is given by

$$\Delta Q_r = m_s C_p \Delta T, \quad (1.11)$$

here m_s is the mass of the substance, ΔT is the temperature differential where the initial temperature of the reaction is subtracted from the final temperature and ΔQ_r is the heat energy taken out or put into the substance.

1.8 Porous medium

A porous medium is characterized by a partitioning of the total volume into solid matrix and pore space, with the latter being filled by one or more fluids. These pores allow the flow of

fluids through the material. The distribution of pores is irregular in nature. Beach sand, human lungs and wood etc. are examples of natural porous media. The features of porous medium is characterized by the Darcy law. Henry Darcy's investigations on steady-state unidirectional flow in a uniform medium revealed a proportionality between flow rate and the applied pressure gradient. This is expressed as

$$u = -\frac{K}{\mu} \nabla \cdot p, \quad (1.12)$$

or

$$\nabla \cdot p = -\frac{\mu}{K} u, \quad (1.13)$$

here $\nabla \cdot p$ is the pressure gradient, K is the permeability of porous medium and μ is the dynamic fluid viscosity. The coefficient K is independent of the nature of the fluid but it depends on the geometry of the medium. Here negative sign indicates that the fluid flows from high pressure to low pressure. Darcy's law is not applicable for $Re > 100$ i.e. for turbulent flows.

1.9 Magnetohydrodynamics

Magnetohydrodynamics is a dynamical branch of the science which deals with a electromagnetic field. Specifically in those matters where currents established by induction modify the field, so the dynamics and field equations are coupled.

Relation between current and drift velocity defined as

$$\mathbf{J} = me \langle \mathbf{v} \rangle. \quad (1.14)$$

Magnetic force so-called Lorentz force defined as:

$$\mathbf{F}_{em} = \mathbf{J} \times \mathbf{B}, \quad (1.15)$$

by Ohm's law

$$\mathbf{J} = \sigma [\mathbf{E} + \mathbf{V} \times \mathbf{B}]. \quad (1.16)$$

When there are no polarization effects we are left with

$$\mathbf{F}_{em} = \sigma [\mathbf{V} \times \mathbf{B}] \times \mathbf{B}. \quad (1.17)$$

In above equations e is the electric charge, n is the number density of electron, \mathbf{J} is the current density, \mathbf{v} is the electrons velocity, σ is the fluid electrical conductivity, \mathbf{B} ($= \mathbf{B}_0 + \mathbf{B}_1$) the total magnetic field, \mathbf{B}_0 is the imposed magnetic field and \mathbf{B}_1 is the induced magnetic field and \mathbf{E} is the electric field. The term $\mathbf{V} \times \mathbf{B}$, in Eqs. (1.15) and (1.16), is due to the Ampere's law. On the basis of Faraday's law, we shall assume that the applied magnetic field is perpendicular to the flow direction.

1.10 Viscous dissipation

The irreversible process by which the work done on the adjacent layers of fluid due to the action of shear forces it is transformed into heat is defined as viscous dissipation. Mathematically

$$\boldsymbol{\tau} \cdot \mathbf{L}, \quad (1.18)$$

where

$$\boldsymbol{\tau} = \begin{bmatrix} \sigma_{xx} & \tau_{xy} & \tau_{xz} \\ \tau_{yx} & \sigma_{yy} & \tau_{yz} \\ \tau_{zx} & \tau_{zy} & \sigma_{zz} \end{bmatrix} \quad (1.19)$$

1.11 Stratification

The phenomenon of changing the state of pressure, temperature, concentration and dissolved substances is responsible for the change in density appeared in the fluid medium is known as stratification. Mathematically, we can write

$$\rho = \rho(x, y, z, t). \quad (1.20)$$

In fluid dynamics, we often studied two types of stratification within the fluid which are described as thermal and solutal stratifications.

1.11.1 Thermal stratification

Thermal stratification appears because of the temperature imbalance, which gives rise to a density imbalance in the fluid medium. When sunlight falls on the lake's surface it changes the temperature. When lake is stratified, three layers are formed within the lake. The upper warm layer referred to as epilimnion and the deeper cold layer referred to as hypolimnion. The boundary layer between the two layers where the temperature changes more rapidly referred to as thermocline. It is also observed that temperature imbalance may alter from one layer to another layer. These flows have wider applications in oceanography and agriculture.

1.11.2 Sloutal stratification

The concentration stratification is applicable to many phenomena like transportation in the sea where stratification occurs due to salinity imbalance. Due to the presence of different fluids, a stable standpoint arises when the lighter fluid stands over the denser one.

1.12 Physical description of dimensionless numbers

All flowing problems have the inertial force (i.e., is the product of mass and acceleration). Besides the inertial force, there exists some additional forces which are responsible for fluid motion. Some dimensionless numbers are discussed below:

1.12.1 Reynolds number

Reynolds number Re is a dimensionless number in a fluid mechanics and heat transfer. It is a measure of the relative importance between the momentum flux by advection and by diffusion in the same direction. It is important to note that velocity and length are taken in the same direction. This suggests that one can present this number based on other advection/diffusion flux ratio defined as

$$\text{Reynolds number} = \frac{\text{Inertial force}}{\text{Viscous force}} = \frac{U_m L}{\nu}. \quad (1.21)$$

Here U_m is the mean velocity, L is a characteristic length and ν is the kinematic viscosity of the fluid.

Reynolds number throws light on the important features of a given flow. Reynolds number is low in the laminar flow and contains viscous effects (forces) dominant, while turbulent flow occurs at high Reynolds number with dominating effects of inertial forces which tend to produce vortices and fluid fluctuates. Reynolds number is larger for air around a car or water around a ship.

1.12.2 Brownian motion parameter

Brownian motion of nanoparticles at the molecular and nanoscale level is a key nanoscale mechanism governing the thermal behavior of nanofluids. Because of the random movement of nanoparticles Brownian motion occurs. Mathematically, it is defined as

$$Nb = \frac{\tau D_B (C_w - C_\infty)}{v}, \quad (1.22)$$

where D_B is the Brownian diffusion coefficient, τ is the ratio of the effective heat capacity of the nanoparticles to heat capacity of the fluid, C_w and C_∞ are respectively the volume fraction of nanoparticles at plate and ambient fluid.

1.12.3 Thermophoresis parameter

A phenomena which transports the nanoparticles from the region of high concentration to the region of low concentration. This factor is observed in mixtures of mobile particles where the different particle exhibit different responses to the force of a temperature gradient. The thermophoresis parameter is defined as

$$Nt = \frac{\tau D_T (T_w - T_\infty)}{v T_\infty}, \quad (1.23)$$

where D_T the thermophoresis diffusion coefficient and T_w and T_∞ are respectively temperature at sheet and ambient medium.

1.12.4 Schmidt number

The Schmidt number is the ratio of thermal diffusion rate to the mass diffusion rate in a fluid. It is analogous to the Prandtl number, which represents the ratio of the momentum diffusivity

to the thermal, defined as

$$Sc = \frac{\text{Thermal diffusion rate}}{\text{Mass diffusion rate}} = \frac{\varpi}{D_B}, \quad (1.24)$$

in above equation ϖ is the thermal diffusivity and D_B is the mass diffusivity.

1.12.5 Prandtl number

Prandtl number is defined as ratio of momentum to thermal diffusivity. Mathematically expressed by

$$Pr = \frac{\text{Momentum diffusivity}}{\text{Thermal diffusivity}} = \frac{\nu}{\varpi}. \quad (1.25)$$

Note that $Pr \ll 1$ corresponds to the case when thermal diffusivity dominates and when $Pr \gg 1$ the momentum diffusivity dominates. In heat transfer and free and forced convection calculations the Prandtl number is often used.

1.12.6 Eckert number

An Eckert number possess a relationship between kinetic energy and enthalpy and accounts for the energy loss due to viscous dissipation. If the role of the momentum energy transferred to thermal energy is significant then Eckert number is to be determined which is defined by

$$Ec = \frac{\text{Kinetic energy}}{\text{Enthalpy}} = \frac{u_c^2}{C_p (T_w - T_\infty)}, \quad (1.26)$$

here u_c is a characteristic velocity of the flow, T_w and T_∞ exhibits the wall and ambient temperature respectively and C_p is the specific heat.

1.12.7 Hartman number

Hartman number is the ratio of magnetic forces to the viscous forces. It is followed by

$$M^2 = \frac{\text{Magnetic forces}}{\text{Viscous forces}} = \frac{B_0^2 L^2}{\mu_m \rho \nu \lambda}. \quad (1.27)$$

In which ρ the density of the fluid, λ the magnetic diffusivity, B_0 is the magnetic field strength, L is the characteristic length and μ_m the magnetic permeability.

1.12.8 Nusselt number

It is the dimensionless quantity that represents the convective to conductive heat transfer coefficients. As transfer of heat by convection and conduction is given by $h(T_w - T_\infty)$ and $k(T_w - T_\infty)/L$. Mathematically

$$Nu = \frac{h(T_w - T_\infty)}{k(T_w - T_\infty)/L} = \frac{hL}{k}, \quad (1.28)$$

wherein k is the thermal conductivity, T_w and T_∞ denote the wall and ambient temperature respectively and h is the heat transfer rate at the wall. In laminar flow, Nusselt number closer to one implies that convection and conduction both are of same magnitude.

1.12.9 Sherwood number

Sherwood number is analogue to Nusselt number. Transfer of mass by convection and diffusion is given by $k(C_w - C_\infty)$ and $D_B(C_w - C_\infty)/L$. It can be expressed mathematically as

$$Sh = \frac{k(C_w - C_\infty)}{D_B(C_w - C_\infty)/L} = \frac{kL}{D_B}, \quad (1.29)$$

here C_w and C_∞ denote the wall and ambient concentration of nanoparticles respectively and D_B is the diffusion coefficient at wall.

1.12.10 Skin friction coefficient

When fluid is passing across a surface then certain amount of drag forces appears. These drag forces are skin friction.

$$C_f = \frac{\tau_w}{\frac{1}{2}\rho u_w^2}, \quad (1.30)$$

where τ_w is the shear stress at the sheet and u_w is the velocity of fluid at sheet. The rise in skin friction tells how much drag attains from the viscous stresses at the boundary. Laminar flow have less drag when compared with turbulent flow. To reduce skin friction it is necessary to convert turbulent flow to laminar flow.

1.13 Constitutive equation

1.13.1 Conservation of mass

For a known velocity profile and no source/sinks it is sufficient to model the continuity equation (flow is continuous, no discontinuity appears through given flow). Conservation of mass hold for physical things. For instance to derive the evolution of the concentration of dust, aerosols or density of a gas, etc. in any medium like air water. Eq. (1.32) represents that the equation of continuity or conservation of mass stems from the principle that mass cannot be created or destroyed inside the control volume. Moreover in the law of conservation of mass total inlet and outlet flux is constant.

$$\frac{\partial \rho}{\partial t} + \nabla \cdot (\rho \mathbf{V}) = 0, \quad (1.31)$$

in which ρ is fluid density, t is time and $\mathbf{V} = (u, v, w)$ the velocity of the moving fluid. The velocity profile for an incompressible fluid reduces to

$$\nabla \cdot \mathbf{V} = 0. \quad (1.32)$$

It will be applicable when there are no inlets or outlets across which fluid can enter or leave the system.

1.13.2 Conservation of linear momentum

It is stated that total linear momentum of an isolated system remains conserved defined by

$$\rho \frac{d\mathbf{V}}{dt} = -\nabla p + \mu \nabla^2 \mathbf{V} + \rho \tilde{\mathbf{b}}. \quad (1.33)$$

Eq. (1.34) expressed the conservation of momentum which states that the total momentum of a closed system of objects (which has no interactions with external agents) is constant. This equation contained the inertial forces which is the internal force on left hand side while on the right hand side the first term term is due to the surface force which is an external force and last two terms are body forces (internal forces).

1.13.3 Conservation of energy

Nanofluid energy equation can be written as

$$\rho C_p \frac{dT}{dt} = -\text{div } \tilde{\mathbf{q}}_r + I_p \nabla \cdot \vec{\mathbf{S}}_p, \quad (1.34)$$

Where I_p is the specific enthalpy of the nanoparticles material, $\vec{\mathbf{S}}_p$ is the nanoparticles diffusion mass flux and $\tilde{\mathbf{q}}_r$ is the energy flux. The first term on left hand side of Eq. (1.34) exhibits the combined effects of change in local energy and advection term. First term displayed on the right hand side comes from Fourier's law of heat conduction and second term is due to nanoparticles. Eq. (1.35) results from the first law of thermodynamics states that the increase in the internal energy of a thermodynamical system is equal to the amount of heat energy added to the system minus the amount of energy lost as a result of the work done by the system on the surroundings. Energy flux is given by

$$\tilde{\mathbf{q}}_r = -k \nabla T + I_p \vec{\mathbf{S}}_p. \quad (1.35)$$

Substituting Eq. (1.35) in Eq. (1.34)

$$\begin{aligned} \rho C_p \frac{dT}{dt} &= -\nabla \cdot (-k \nabla T + I_p \vec{\mathbf{S}}_p) + I_p \nabla \cdot \vec{\mathbf{S}}_p, \\ &= k \nabla^2 T - \nabla \cdot (I_p \vec{\mathbf{S}}_p) + I_p \nabla \cdot \vec{\mathbf{S}}_p, \\ &= k \nabla^2 T - I_p \nabla \cdot \vec{\mathbf{S}}_p - \vec{\mathbf{S}}_p \cdot \nabla I_p + I_p \nabla \cdot \vec{\mathbf{S}}_p, \\ &= k \nabla^2 T - \vec{\mathbf{S}}_p \cdot \nabla I_p. \end{aligned} \quad (1.36)$$

As vector identity is

$$\nabla I_p = C_p \nabla T, \quad (1.37)$$

one obtains from Eq. (1.37)

$$\rho C_p \frac{dT}{dt} = k \nabla^2 T - C_p \vec{\mathbf{S}}_p \cdot \nabla T. \quad (1.38)$$

Diffusion mass flux \vec{S}_p for the nanoparticles, given as the sum of two diffusion terms (Brownian diffusion and thermophoresis) by

$$\vec{S}_p = \vec{S}_{p,B} + \vec{S}_{p,T}, \quad (1.39)$$

with

$$\vec{S}_{p,B} = -\rho_p D_B \nabla C, \quad (1.40)$$

Here Brownian diffusion coefficient D_B can be defined by the Einstein-Stokes equation

$$D_B = \frac{k_B T}{3\pi\mu d_p}, \quad (1.41)$$

in which k_B is the Boltzmann's constant and d_p is the nanoparticles diameter.

$$\vec{S}_{p,T} = \rho_p C \tilde{V}_\tau, \quad (1.42)$$

$$\tilde{V}_\tau = -\tilde{\gamma} \frac{\mu}{\rho} \frac{\nabla T}{T}, \quad (1.43)$$

for the thermophoresis velocity \tilde{V}_τ . In above equation, the proportionality factor $\tilde{\gamma}$ while ρ_p and ρ are the densities of nanoparticles and base fluid respectively can be expressed as follows:

$$\tilde{\gamma} = 0.26 \frac{k}{2k + k_p}, \quad (1.44)$$

in which k_p and k are the thermal conductivities of the the particle material respectively and fluid. Hence the thermophoresis diffusion flux is given by

$$\vec{S}_{p,T} = -\rho_p D_T \frac{\nabla T}{T}, \quad (1.45)$$

Where

$$D_T = \frac{\tilde{\gamma} \mu C}{\rho}, \quad (1.46)$$



which is the thermophoresis diffusion coefficient. From Eq. (1.40) and (1.45), diffusion mass flux is given by

$$\vec{S}_p = -\rho_p D_B \nabla C - \rho_p D_T \frac{\nabla T}{T} \quad (1.47)$$

Thus Eq. (1.38) becomes

$$\rho C_p \frac{dT}{dt} = k \nabla^2 T + \rho_p C_p \left[D_B \nabla C \cdot \nabla T + D_T \frac{\nabla T \cdot \nabla T}{T} \right], \quad (1.48)$$

which is the nanofluid energy equation.

1.13.4 Conservation of concentration

For the nanoparticles the concentration equation is

$$\frac{\partial C}{\partial t} + \vec{V} \cdot \nabla C = -\frac{1}{\rho_p} \nabla \cdot \vec{S}_p, \quad (1.49)$$

where ρ_p is the mass density of the nanoparticles, C is nanoparticles volume fraction and \vec{S}_p is the diffusion mass flux. Now using the Eq. (1.47), we get

$$\frac{\partial C}{\partial t} + \vec{V} \cdot \nabla C = \nabla \cdot \left[D_B \nabla C + D_T \frac{\nabla T}{T} \right], \quad (1.50)$$

which is the concentration equation for nanofluids. Fick's first and second laws, known as law of conservation of concentration gave his contribution to find out the Eq. (1.51).

1.14 Solution methodology

In the field of science and engineering, specifically in the fluid mechanics many problems are non-linear. It is very difficult and some times even impossible to compute the exact solution of these non-linear problems. To get rid of this problem scientists have found successful analytical and numerical techniques. Among all of them HAM is the most convenient analytical technique to use. To get the analytical and series solutions of non-linear governing equations we have captured this technique in the upcoming chapters.

1.14.1 Homotopy analysis method

The concept of homotopy was first formulated by Poincare around 1900 (Collins 2004). In topology, two functions are called homotopic if one can be "continuously deformed" into the other. Homotopy is a combination of two Greek words homos means identical and topos means place. If there exists two continuous mapping g_1 and g_2 from the topological space S into the topological space Z resulting g_1 is homotopic to g_2 . A continuous mapping G exists then

$$G : S \times [0, 1] \rightarrow Z, \quad (1.51)$$

such that for each $s \in S$

$$G(s, 0) = g_1(s), \quad G(s, 1) = g_2(s). \quad (1.52)$$

The mapping G is called the homotopy between g_1 and g_2 .



Chapter 2

Boundary layer nanofluid flow past a stretching sheet

This chapter develops the steady two-dimensional flow of viscous nanofluid over a stretchable surface. The nonlinear ordinary differential equations are obtained by using the usual suitable transformations. The resulting equations are solved analytically by using homotopy analysis method (HAM). Influence of different physical parameters such as Brownian motion parameter Nb , thermophoresis parameter Nt , Schmidt number Sc and Prandtl number Pr on temperature and concentration profiles are examined with the help of graphs. Numerical values of heat and mass transfer coefficients are presented in tables.

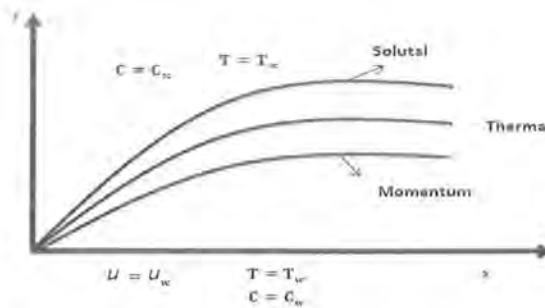


Figure 2.1: Geometry of the flow.

2.1 Mathematical formulation

Here we inquired the two dimensional viscous nanofluid flow over a stretchable surface is with linear stretching velocity $u_w(x) = ax$, where a is a constant and x is the coordinate axis. The disturbance is generated in a fluid flow by the stretchable surface. The mechanical properties of the final product strictly depend on the stretching rate and the rate of cooling in this process. The fluid flow is confined to $y > 0$, where y coordinate is measured perpendicular to the stretching surface. The surface of stretching sheet is maintained at uniform temperature T_w whereas the temperature far away from the surface is T_∞ . Under the influence of these assumptions, the governing equations can be written as follows:

$$\frac{\partial u}{\partial x} + \frac{\partial v}{\partial y} = 0, \quad (2.1)$$

$$\rho \left(u \frac{\partial u}{\partial x} + v \frac{\partial u}{\partial y} \right) = \mu \frac{\partial^2 u}{\partial y^2}, \quad (2.2)$$

$$u \frac{\partial T}{\partial x} + v \frac{\partial T}{\partial y} = \frac{k}{(\rho C_p)_f} \left(\frac{\partial^2 T}{\partial y^2} \right) + \frac{(\rho C_p)_p}{(\rho C_p)_f} \left[D_B \left(\frac{\partial C}{\partial y} \frac{\partial T}{\partial y} \right) + \frac{D_T}{T_\infty} \left(\frac{\partial T}{\partial y} \right)^2 \right], \quad (2.3)$$

$$u \frac{\partial C}{\partial x} + v \frac{\partial C}{\partial y} = D_B \left(\frac{\partial^2 C}{\partial y^2} \right) + \frac{D_T}{T_\infty} \left(\frac{\partial^2 T}{\partial y^2} \right). \quad (2.4)$$

In above equations, u and v represent the respective velocity components in x - and y -directions, T the temperature, C the volume fraction of nanoparticles, k the thermal conductivity of fluid, ρ the fluid density, μ the effective kinematic viscosity of the fluid, $(\rho C_p)_p$ and $(\rho C_p)_f$ are the heat capacity of nanoparticles material and fluid, D_B and D_T are the Brownian diffusion coefficient and the thermophoresis diffusion coefficient of the nanofluid.

The appropriate boundary conditions are given by

$$\begin{aligned} u &= u_w(x) = ax, \quad v = 0, \quad T = T_w, \quad C = C_w \quad \text{at } y = 0, \\ u &= v = 0, \quad T = T_\infty, \quad C = C_\infty \quad \text{at } y \rightarrow \infty. \end{aligned} \quad (2.5)$$



We introduce the subsequent similarity transformations:

$$\psi = (av)^{\frac{1}{2}} x f(\eta), \quad \theta(\eta) = \frac{T - T_{\infty}}{T_w - T_{\infty}}, \quad \phi(\eta) = \frac{C - C_{\infty}}{C_w - C_{\infty}}, \quad \eta = \left(\frac{a}{\nu}\right)^{\frac{1}{2}} y, \quad (2.6)$$

in which ψ is the stream function defined in the usual way as $u = \frac{\partial \psi}{\partial y}$ and $v = -\frac{\partial \psi}{\partial x}$.

Using Eq. (2.6), the continuity equation (2.1) is automatically satisfied while Eqs. (2.2) – (2.4) reduced to

$$f''' - f'^2 + ff'' = 0, \quad (2.7)$$

$$\frac{1}{\text{Pr}} \theta'' + f\theta' + Nb\theta'\phi' + Nt\theta'^2 = 0, \quad (2.8)$$

$$\phi'' + Scf\phi' + \frac{Nt}{Nb}\theta'' = 0, \quad (2.9)$$

together with the boundary conditions

$$\begin{aligned} f(0) &= 0, \quad f'(0) = 1, \quad \theta(0) = 1, \quad \phi(0) = 1, \\ f'(\infty) &= 0, \quad \theta(\infty) = 0, \quad \phi(\infty) = 0. \end{aligned} \quad (2.10)$$

Note that the prime on the quantities represents the differentiation with respect to η . Moreover, the non-dimensional constants appearing in Eqs. (2.7) – (2.9) are the Prandtl number Pr , thermophoresis parameter Nt , Schmidt number Sc and Brownian motion parameter Nb . These are respectively defined by

$$\text{Pr} = \frac{\nu}{\alpha}, \quad Nb = \frac{(\rho C)_p D_B (C_w - C_{\infty})}{(\rho C)_f \nu}, \quad Sc = \frac{\nu}{D_B}, \quad Nt = \frac{(\rho C)_p D_T (T_w - T_{\infty})}{(\rho C)_f T_{\infty} \nu}. \quad (2.11)$$

The local Nusselt and Sherwood numbers in non-dimensional form can be written as

$$Nu = \frac{xq_w}{k(T_w - T_{\infty})}, \quad Sh = \frac{xq_m}{D_B(C_w - C_{\infty})}, \quad (2.12)$$

where q_w and q_m are the wall heat and mass fluxes, respectively are given by

$$q_w = -k \left. \frac{\partial T}{\partial y} \right|_{y=0}, \quad q_m = -D_B \left. \frac{\partial C}{\partial y} \right|_{y=0}, \quad (2.13)$$

By utilization of above equation, we get

$$(\text{Re}_x)^{-\frac{1}{2}} Nu = -\theta'(0), \quad (\text{Re}_x)^{-\frac{1}{2}} Sh = -\phi'(0), \quad (2.14)$$

where $(\text{Re}_x)^{\frac{1}{2}} = ax/\nu$ is the local Reynolds number.

The exact solution of Eq. (2.7) along with (2.10) has been obtained by Pop [12] and can be written as

$$f(\eta) = 1 - \exp(-\eta) \quad (2.15)$$

2.2 Homotopy solution

For homotopic solutions, we select some initial guesses and the linear operators \mathcal{L}_i ($i = 1 - 2$) in the form

$$\theta_0(\eta) = e^{-\eta}, \quad \phi_0(\eta) = e^{-\eta}, \quad (2.16)$$

$$\mathcal{L}_\theta = \theta'' - \theta, \quad \mathcal{L}_\phi = \phi'' - \phi. \quad (2.17)$$

The above operators satisfy the following properties

$$\mathcal{L}_\theta(B_1 e^\eta + B_2 e^{-\eta}) = 0, \quad (2.18)$$

$$\mathcal{L}_\phi(B_3 e^\eta + B_4 e^{-\eta}) = 0, \quad (2.19)$$

here the calculated arbitrary constants are B_i ($i = 1 - 4$).

2.2.1 Zeroth order deformation equations

The defined zeroth-order deformation equations and \hbar_θ and \hbar_ϕ are embedded parameters for the given problem are

$$(1 - p) \mathcal{L}_\theta [\tilde{\theta}(\eta; p) - \theta_0(\eta)] = p \hbar_\theta \mathcal{N}_\theta [\tilde{\theta}(\eta; p), \tilde{f}(\eta; p), \tilde{\phi}(\eta; p)], \quad (2.20)$$

$$\tilde{\theta}(0; p) = 1, \quad \tilde{\theta}(\infty; p) = 0, \quad (2.21)$$

$$(1 - p) \mathcal{L}_\phi [\tilde{\phi}(\eta; p) - \phi_0(\eta)] = p \hbar_\phi \mathcal{N}_\phi [\tilde{\phi}(\eta; p), \tilde{\theta}(\eta; p), \tilde{f}(\eta; p)], \quad (2.22)$$



$$\tilde{\phi}(0; p) = 1, \quad \tilde{\phi}(\infty; p) = 0, \quad (2.23)$$

The pertinent nonlinear operators $\mathcal{N}_{\tilde{\theta}}[\tilde{\theta}(\eta; p)]$ and $\mathcal{N}_{\tilde{\phi}}[\tilde{\phi}(\eta; p)]$ are given by

$$\begin{aligned} \mathcal{N}_{\tilde{\theta}}[\tilde{\theta}(\eta; p), \tilde{f}(\eta; p), \tilde{\phi}(\eta; p)] &= \frac{1}{\text{Pr}} \frac{\partial^2 \tilde{\theta}(\eta; p)}{\partial \eta^2} + Nb \frac{\partial \tilde{\theta}(\eta; p)}{\partial \eta} \frac{\partial \tilde{\phi}(\eta; p)}{\partial \eta} \\ &\quad + \tilde{f}(\eta; p) \frac{\partial \tilde{\theta}(\eta; p)}{\partial \eta} + Nt \left(\frac{\partial \tilde{\theta}(\eta; p)}{\partial \eta} \right)^2, \end{aligned} \quad (2.24)$$

$$\mathcal{N}_{\tilde{\phi}}[\tilde{\phi}(\eta; p), \tilde{\theta}(\eta; p), \tilde{f}(\eta; p)] = \frac{\partial^2 \tilde{\phi}(\eta; p)}{\partial \eta^2} + Sc \tilde{f}(\eta; p) \frac{\partial \tilde{\phi}(\eta; p)}{\partial \eta} + \frac{Nt}{Nb} \frac{\partial^2 \tilde{\theta}(\eta; p)}{\partial \eta^2}, \quad (2.25)$$

where p changes from 0 to 1, then $\tilde{\theta}(\eta, p)$ varies from $\theta_0(\eta)$ to $\theta(\eta)$ and $\tilde{\phi}(\eta, p)$ varies from $\phi_0(\eta)$ to $\phi(\eta)$, respectively.

$$\tilde{\theta}(\eta; 0) = \theta_0(\eta), \quad \tilde{\theta}(\eta; 1) = \theta(\eta), \quad (2.26)$$

$$\tilde{\phi}(\eta; 0) = \phi_0(\eta), \quad \tilde{\phi}(\eta; 1) = \phi(\eta). \quad (2.27)$$

In view of Taylor's series

$$\begin{aligned} \tilde{\theta}(\eta; p) &= \theta_0(\eta) + \sum_{m=1}^{\infty} \theta_m(\eta) p^m; \quad \theta_m(\eta) = \frac{1}{m!} \frac{\partial^m \tilde{\theta}(\eta; p)}{\partial p^m} \Big|_{p=0}, \\ \tilde{\phi}(\eta; p) &= \phi_0(\eta) + \sum_{m=1}^{\infty} \phi_m(\eta) p^m; \quad \phi_m(\eta) = \frac{1}{m!} \frac{\partial^m \tilde{\phi}(\eta; p)}{\partial p^m} \Big|_{p=0}, \end{aligned} \quad (2.28)$$

Thus

$$\begin{aligned} \theta(\eta) &= \theta_0(\eta) + \sum_{m=1}^{\infty} \theta_m(\eta), \\ \phi(\eta) &= \phi_0(\eta) + \sum_{m=1}^{\infty} \phi_m(\eta). \end{aligned} \quad (2.29)$$

2.2.2 Deformation problems of mth-order

The mth order problems are given by

$$\mathcal{L}_\theta [\theta_m(\eta) - \chi_m \theta_{m-1}(\eta)] = \hbar_\theta \mathcal{R}_m^\theta(\eta), \quad (2.30)$$

$$\theta_m(0) = \theta_m(\infty) = 0, \quad (2.31)$$

$$\mathcal{L}_\phi [\phi_m(\eta) - \chi_m \phi_{m-1}(\eta)] = \hbar_\phi \mathcal{R}_m^\phi(\eta), \quad (2.32)$$

$$\phi_m(0) = \phi_m(\infty) = 0, \quad (2.33)$$

in which

$$\mathcal{R}_m^\theta(\eta) = \frac{1}{\text{Pr}} \theta_{m-1}''(\eta) + \sum_{k=0}^{m-1} [f_{m-1-k} \theta_k' + Nb \phi_{m-1-k}' \theta_k' + Nt \theta_{m-1-k}' \theta_k'], \quad (2.34)$$

$$\mathcal{R}_m^\phi(\eta) = \left[\phi_{m-1}''(\eta) + Sc \sum_{k=0}^{m-1} f_{m-1-k} \phi_k' + \frac{Nt}{Nb} \theta_{m-1}'' \right], \quad (2.35)$$

$$\chi_m = \begin{cases} 0, & m \leq 1, \\ 1, & m > 1, \end{cases} \quad (2.36)$$

The general solutions are

$$\theta_m(\eta) = \theta_m^*(\eta) + B_1 e^\eta + B_2 e^{-\eta}, \quad (2.37)$$

$$\phi_m(\eta) = \phi_m^*(\eta) + B_3 e^\eta + B_4 e^{-\eta}, \quad (2.38)$$

2.3 Convergence of HAM solution

Homotopy analysis method (HAM) involves embedding parameter \hbar which play a vital role to control the convergence of the series solution. The suitable range for admissible values of \hbar can be evaluated by sketching the \hbar -curves for temperature and concentration fields as displayed in Figure (2.2). It is clear that the acceptable values of \hbar_θ and \hbar_ϕ lie in the range $[-1.4, -0.4]$ for some fixed values of the other involved parameters. We further observed that the series solutions have convergence in the entire region of η ($0 < \eta < \infty$) when $\hbar_\theta = \hbar_\phi = -0.9$.



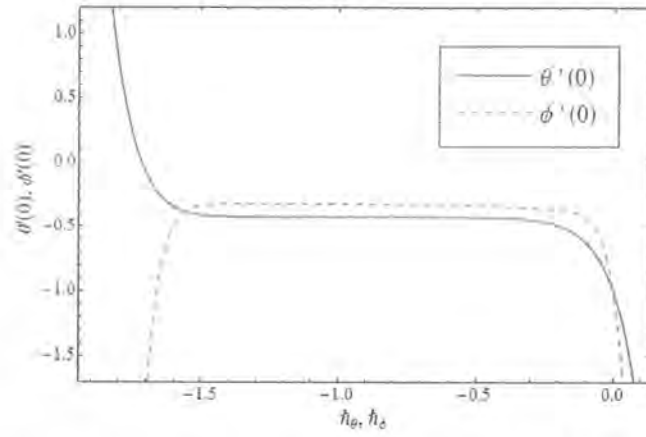


Figure 2.2: Combined h -curves for $\theta'(0)$ and $\phi'(0)$.

Table 2.1: Order of approximations for the HAM solutions when $Pr = 1.3$, $Nb = Nt = 0.2$ and $Sc = 1.0$.

Order of approximations	$-\theta'(0)$	$-\phi'(0)$
1	0.54333	0.16666
5	0.56869	0.23492
10	0.57311	0.20227
15	0.57307	0.20223
21	0.57308	0.20223
25	0.57308	0.20223
30	0.57308	0.20223
35	0.57308	0.20223
40	0.57308	0.20223
45	0.57308	0.20223
50	0.57308	0.20223
55	0.57308	0.20223

2.4 Results and discussion

Variation of pertinent parameters on the temperature profile $\theta(\eta)$ is sketched in Figures (2.3 – 2.5). In particular, the influence of increasing Brownian motion parameter Nb on temperature profile $\theta(\eta)$ is shown in Figure (2.3). It is evident that an increase in Nb corresponds to an increase in the temperature profile. Due to the fact that Brownian motion is responsible for random motion of nanoparticles in base fluid. So with increasing values of Nb , nanoparticles vibrate haphazardly and temperature profile increases. The variation of thermophoresis parameter Nt on $\theta(\eta)$ is depicted in Figure (2.4). It reveals that by increasing the values of thermophoresis parameter Nt , the temperature profile $\theta(\eta)$ and thermal boundary layer thickness also increases. We concluded from Figure (2.5) that an increment in the Prandtl number Pr provides a rapid reduction in the thermal diffusivity hence the temperature decreases.

Figures (2.6 – 2.8) demonstrate the variation of embedded parameters on nanoparticles concentration. With an increase in Brownian motion parameter Nb , concentration profile decreases as evident from Figure (2.6). In Figure (2.7) we encountered variation of concentration profile $\phi(\eta)$ corresponding to the increasing values of thermophoresis parameter Nt . Here we noticed that the concentration profile $\phi(\eta)$ increases via thermophoresis parameter Nt . Effects of Sc on concentration profile $\phi(\eta)$ are captured in Figure (2.8) where a decrease in the concentration profile $\phi(\eta)$ is noted with the increasing value of Sc .

Table (2.1) is prepared to give the convergence of series solution. Convergence is achieved at 21^{st} —order of approximations. The numerical values of dimensionless heat and mass transfer rates for different values of embedded parameters such as Nt , Nb , Sc and Pr are given in Table 2.2. Analysis of Table (2.2) reveals that there is a decrease in the heat transfer rate when there is an increase in Nb , Nt and Sc while it increases with the increasing values of Prandtl number Pr . The effects of Nt , Nb and Sc on the dimensionless mass rate exhibit an increasing behavior whereas the effect of Pr is to decrease the mass rate.

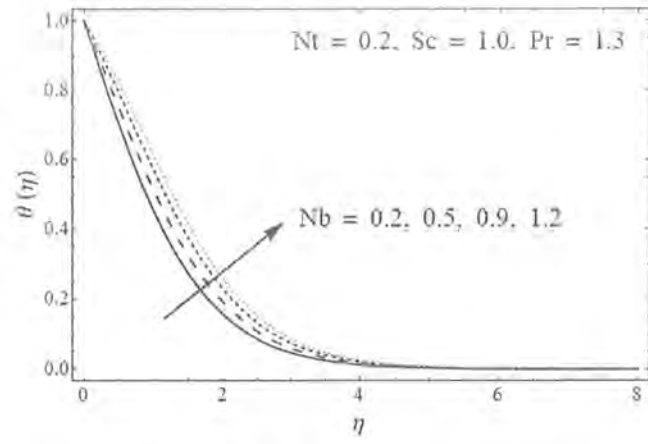


Figure 2.3: Impact of Nb on temperature $\theta(\eta)$.

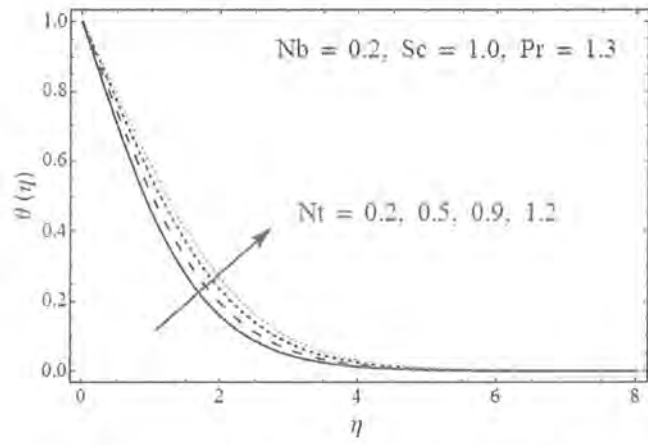


Figure 2.4: Impact of Nt on temperature $\theta(\eta)$.

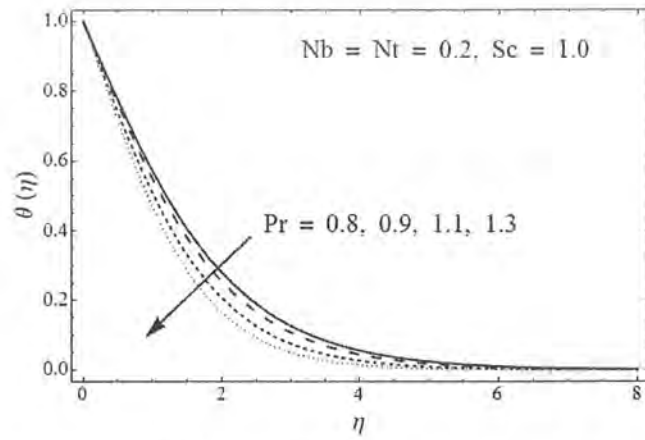


Figure 2.5: Impact of Pr on temperature $\theta(\eta)$.

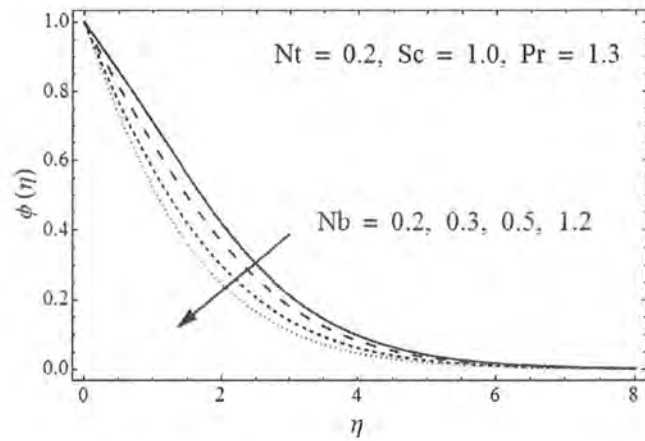


Figure 2.6: Impact of Nb on concentration $\phi(\eta)$.



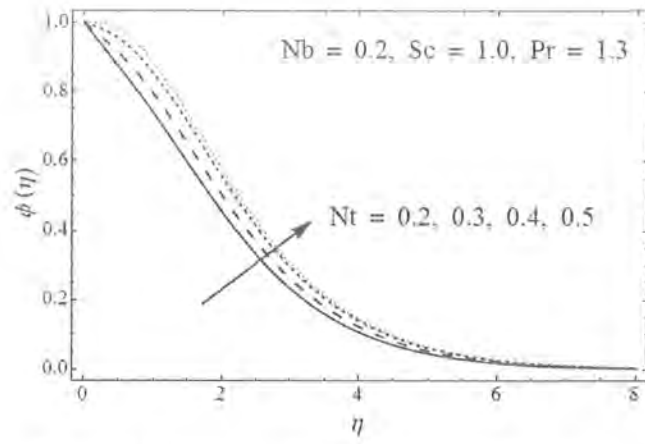


Figure 2.7: Impact of Nt on concentration $\phi(\eta)$.

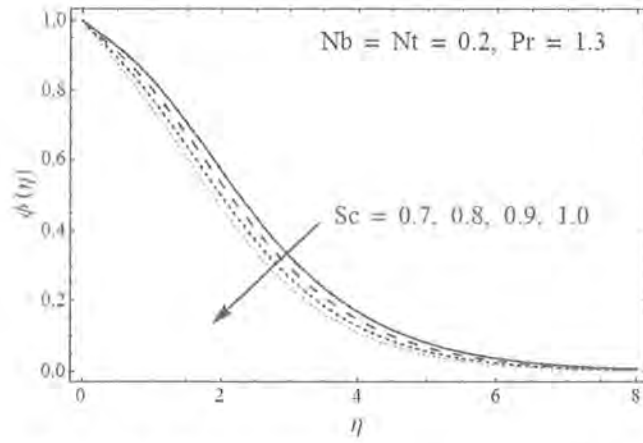


Figure 2.8: Impact of Sc on concentration $\phi(\eta)$.

Table 2.2: Numerical values of Nusselt and Sherwood numbers when $Pr = 1.3$, $Nt = Nb = 0.2$ and $Sc = 1.0$.

Nb	Nt	Sc	Pr	$-\theta'(0)$	$-\phi'(0)$
0.2	0.2	1.0	1.3	0.57308	0.20223
0.3				0.53864	0.34832
0.4				0.50564	0.42068
0.6				0.44392	0.49166
	0.3			0.55317	0.03695
	0.4			0.53406	0.11478
	0.6			0.49188	0.37780
		0.9		0.57820	0.13729
		1.1		0.56853	0.25392
		1.2		0.56444	0.30279
			0.7	0.39971	0.32672
			1.0	0.49544	0.25891
			1.2	0.54879	0.22012

2.5 Key findings

The determination of our work is to venture in the regime of flow of mass and heat transfer of a nanofluid past a stretchable surface. Analytical solutions are presented for temperature and concentration profiles. Effects of different parameter such as Brownian motion parameter Nb , thermophoresis parameter Nt , Prandtl number Pr and Schmidt number Sc are discussed through graphical illustrations. For larger values of Nb and Nt , temperature grows up while it decays for Pr . Similarly volume fraction of nanoparticles decreases against the Schmidt number Sc . Brownian and thermophoresis parameters have an opposite effect on the concentration field. The wall temperature gradient increases with an increase in Pr . Also local Sherwood number enhances by increasing Nb , Nt and Sc .

Chapter 3

MHD effects on thermo-solutal stratified nanofluid flow by an exponential stretching sheet with thermal radiation

Here the analysis of previous chapter is extended for steady boundary layer flow of nanofluid past an exponential stretchable surface. Heat and mass transfer phenomenon is examined under the influence of double stratified medium. Effects of porous medium and thermal radiation are also encountered. By taking the suitable similarity transformations the governing partial differential equations are transformed to a system of nonlinear ordinary differential equations. Homotopy analysis method (HAM) is utilized to solve the arising mathematical problem. Impact of pertinent parameters through graphical illustrations are investigated. It is noted that thermal and solutal stratification parameters are in the favour of rate of heat and mass transfer.

3.1 Problem formulation

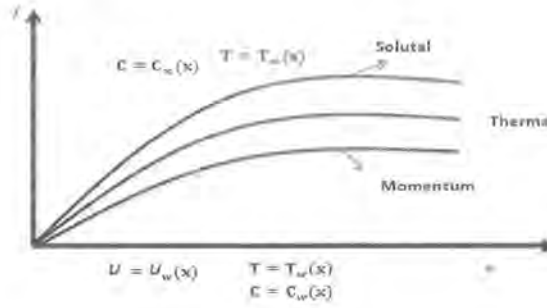


Figure 3.1: Geometry of the problem.

Here we consider the steady Newtonian (viscous) flow of nanofluid beyond a exponential stretched surface immersed in a thermal and solutal stratified medium. An incompressible fluid saturates the porous medium. Surface is stretched along x -axis and the flow is confined to $y > 0$. Due to the exponential stretching sheet a boundary layer arises having the dominant viscous effects across the fluid. The velocity of the stretched surface is $u_w(x) = U_0 e^{\frac{x}{2L}}$. By Darcy's Law, the porous medium features have been characterized. The Buongiorno's nanofluid model incorporates the Brownian motion and thermophoresis impacts. The magnetic field having strength B_0 is applied to the fluid flow in the transverse direction. Under the assumption of small magnetic Reynolds number, induced magnetic field is ignored. The temperature and concentration at sheet and far away from the sheet are assumed to be exponentially stratified in the forms $T_w(x) = T_0 + be^{\frac{x}{2L}}$, $C_w(x) = C_0 + ae^{\frac{x}{2L}}$ and $T_\infty(x) = T_0 + ce^{\frac{x}{2L}}$, $C_\infty(x) = C_0 + de^{\frac{x}{2L}}$ respectively (with a , b , c , and d the constants). Using the boundary layer approximations, the governing equations for nanofluid are given by

$$\frac{\partial u}{\partial x} + \frac{\partial v}{\partial y} = 0, \quad (3.1)$$

$$\rho \left(u \frac{\partial u}{\partial x} + v \frac{\partial u}{\partial y} \right) = \mu \frac{\partial^2 u}{\partial y^2} - \frac{\mu}{K} u - \sigma B_0^2 u, \quad (3.2)$$

$$u \frac{\partial T}{\partial x} + v \frac{\partial T}{\partial y} = \frac{k}{(\rho C_p)_f} \left(\frac{\partial^2 T}{\partial y^2} \right) + \frac{(\rho C_p)_p}{(\rho C_p)_f} \left[D_B \left(\frac{\partial C}{\partial y} \frac{\partial T}{\partial y} \right) + \frac{D_T}{T_\infty} \left(\frac{\partial T}{\partial y} \right)^2 \right] + \frac{16\sigma^* T_\infty^3}{k^* (\rho C_p)_f} \frac{\partial^2 T}{\partial y^2} + \frac{\mu}{(\rho C_p)_f} \left(\frac{\partial u}{\partial y} \right)^2, \quad (3.3)$$

$$u \frac{\partial C}{\partial x} + v \frac{\partial C}{\partial y} = D_B \left(\frac{\partial^2 C}{\partial y^2} \right) + \frac{D_T}{T_\infty} \left(\frac{\partial^2 T}{\partial y^2} \right). \quad (3.4)$$

In above equations, u and v represent the respective velocity components in x - and y -directions, T the temperature, C the concentration of nanoparticles, D_B and D_T are the Brownian and thermophoresis diffusion coefficient of the nanofluid, ρ the fluid density, μ the effective kinematic viscosity of the fluid, k the thermal conductivity of fluid and $(\rho C_p)_p$ and $(\rho C_p)_f$ are the heat capacities of nanoparticles material and nanofluid. Rosseland approximation leads to the given expression:

$$q_r = -\frac{4\sigma}{3k^*} \frac{\partial T^4}{\partial y}, \quad (3.5)$$

where k^* the absorption coefficient while σ the Stefan Boltzman constant. On the expansion of Taylor series we are left with

$$T^4 \approx 4T_\infty^3 T - 3T_\infty^4. \quad (3.6)$$

The appropriate conditions are given by

$$\begin{aligned} u &= u_w = U_0 e^{\frac{x}{2L}}, \quad v = 0, \quad T = T_w = T_0 + b e^{\frac{x}{2L}}, \quad C = C_w = C_0 + a e^{\frac{x}{2L}} \text{ at } y = 0, \\ u, v &\rightarrow 0, \quad T = T_\infty = T_0 + c e^{\frac{x}{2L}}, \quad C = C_\infty = C_0 + d e^{\frac{x}{2L}} \text{ when } y \rightarrow \infty. \end{aligned} \quad (3.7)$$

Considering

$$\begin{aligned} \eta &= y \sqrt{\frac{U_0}{2\nu L}} e^{\frac{x}{2L}}, \quad v = -\sqrt{\frac{\nu U_0}{2L}} e^{\frac{x}{2L}} [f(\eta) + \eta f'(\eta)], \\ u &= U_0 e^{\frac{x}{2L}} f'(\eta), \quad \theta(\eta) = \frac{T - T_\infty}{T_w - T_0}, \quad \phi(\eta) = \frac{C - C_\infty}{C_w - C_0}. \end{aligned} \quad (3.8)$$

Eq. (3.1) is identically satisfied and Eqs. (3.2) – (3.4) and (3.7) gives

$$f''' - (M + \lambda) f' - 2f'^2 + f f'' = 0, \quad (3.9)$$



$$\frac{1}{\text{Pr}} \left(1 + \frac{4}{3} R \right) \theta'' + Nb \theta' \phi' + Nt \theta'^2 + Ec f''^2 - St f' - f' \theta + \theta' f = 0, \quad (3.10)$$

$$\phi'' + \frac{Nt}{Nb} \theta'' + Sc (f \phi' - f' \phi) - Sc Sm f' = 0, \quad (3.11)$$

$$f'(0) = 1, \quad f(0) = 0, \quad f'(\infty) = 0, \quad (3.12)$$

$$\theta(0) = 1 - St, \quad \theta(\infty) = 0, \quad (3.13)$$

$$\phi(0) = 1 - Sm, \quad \phi(\infty) = 0, \quad (3.14)$$

where similarity variable is η and $f'(\eta)$, $\theta(\eta)$ and $\phi(\eta)$ are the dimensionless velocity, temperature and concentration. Moreover the different parameters namely the Hartman number M , Prandtl number Pr , porosity parameter λ , radiation parameter R , Eckert number Ec , Brownian motion parameter Nb , thermophoresis parameter Nt , thermal stratified parameter St , solutal stratified parameter Sm and Schmidt number Sc are defined by

$$\begin{aligned} M &= \frac{2\sigma B_0^2 L}{\rho U_0}, \quad \text{Pr} = \frac{\nu(\rho C_p)_f}{k}, \quad \lambda = \frac{\nu L}{K U_0} e^{-\frac{x}{L}}, \quad R = \frac{4\sigma^* T_\infty^3}{k^* k}, \\ Ec &= \frac{U_0^2 e^{\frac{2x}{L}}}{be^{\frac{x}{2L}}(\rho C_p)_f}, \quad Nb = \frac{\tau D_B (C_w - C_0)}{\nu}, \quad Nt = \frac{\tau D_T (T_w - T_0)}{\nu T_\infty}, \\ St &= \frac{c}{b}, \quad Sm = \frac{d}{a}, \quad Sc = \frac{\nu}{D_B}. \end{aligned} \quad (3.15)$$

Local Nusselt number Nu , skin-friction coefficient C_f and Sherwood number Sh are given by

$$Nu = -\frac{x q_w}{k(T_w - T_\infty)}, \quad C_f = \frac{\tau_w|_{y=0}}{\frac{1}{2}\rho U_0^2 e^{\frac{2x}{L}}}, \quad Sh = -\frac{x q_m}{D_B(C_w - C_\infty)}, \quad (3.16)$$

$$\begin{aligned} Nu \text{Re}_x^{-1/2} \sqrt{\frac{2L}{x}} &= -\left(1 + \frac{4R}{3}\right) \left(\frac{1}{1 - St}\right) \theta'(0), \quad C_f \sqrt{\frac{\text{Re}_x}{2}} = f''(0), \\ Sh \text{Re}_x^{-1/2} \sqrt{\frac{2L}{x}} &= -\left(\frac{1}{1 - Sm}\right) \phi'(0), \end{aligned} \quad (3.17)$$

the above equations contain local Reynolds number defined as $(\text{Re}_x)^{\frac{1}{2}} = U_0 e^{\frac{x}{L}} / \nu$.



3.2 Homotopy solution

By the utilization of homotopy analysis method the series solution is computed which requires the linear operators \mathcal{L}_f , \mathcal{L}_θ and \mathcal{L}_ϕ and the initial guesses $f_0(\eta)$, $\theta_0(\eta)$ and $\phi_0(\eta)$ in the forms:

$$f_0(\eta) = 1 - \exp(-\eta), \quad \theta_0(\eta) = (1 - St) \exp(-\eta), \quad \phi_0(\eta) = (1 - Sm) \exp(-\eta), \quad (3.18)$$

$$\mathcal{L}_f(f) = f''' - f', \quad \mathcal{L}_\theta(\theta) = \theta'' - \theta, \quad \mathcal{L}_\phi(\phi) = \phi'' - \phi, \quad (3.19)$$

with the properties

$$\begin{aligned} \mathcal{L}_f [D_1 + D_2 \exp(-\eta) + D_3 \exp(\eta)] &= 0, \\ \mathcal{L}_\theta [D_4 \exp(-\eta) + D_5 \exp(\eta)] &= 0, \\ \mathcal{L}_\phi [D_6 \exp(-\eta) + D_7 \exp(\eta)] &= 0, \end{aligned} \quad (3.20)$$

above equations contain arbitrary constants defined as D_i ($i = 1 - 7$).

3.2.1 Zeroth order deformation equations

Let \hbar_f , \hbar_θ and \hbar_ϕ are the non-zero auxiliary parameters then we form the zeroth-order deformation problems as:

$$(1 - p) \mathcal{L}_f [\tilde{f}(\eta; p) - f_0(\eta)] = p \hbar_f \mathcal{N}_f [\tilde{f}(\eta; p)], \quad (3.21)$$

$$\tilde{f}(0; p) = 0, \quad \tilde{f}'(0; p) = 1, \quad \tilde{f}'(\infty; p) = 0, \quad (3.22)$$

$$(1 - p) \mathcal{L}_\theta [\tilde{\theta}(\eta; p) - \theta_0(\eta)] = p \hbar_\theta \mathcal{N}_\theta [\tilde{\theta}(\eta; p), \tilde{\phi}(\eta; p), \tilde{f}(\eta; p)], \quad (3.23)$$

$$\tilde{\theta}(0; p) = 1 - St, \quad \tilde{\theta}(\infty; p) = 0, \quad (3.24)$$

$$(1 - p) \mathcal{L}_\phi [\tilde{\phi}(\eta; p) - \phi_0(\eta)] = p \hbar_\phi \mathcal{N}_\phi [\tilde{\phi}(\eta; p), \tilde{f}(\eta; p), \tilde{\theta}(\eta; p)], \quad (3.25)$$

$$\tilde{\phi}(0; p) = 1 - Sm, \quad \tilde{\phi}(\infty; p) = 0. \quad (3.26)$$

The definitions of the non-linear operator $\mathcal{N}_f [\tilde{f}(\eta; p)]$, $\mathcal{N}_\theta [\tilde{\theta}(\eta; p)]$ and $\mathcal{N}_\phi [\tilde{\phi}(\eta; p)]$ of Eqs. (3.9) – (3.11) are

$$\mathcal{N}_f [\tilde{f}(\eta; p)] = \frac{\partial^3 \tilde{f}(\eta; p)}{\partial \eta^3} - (M + \lambda) \frac{\partial \tilde{f}(\eta; p)}{\partial \eta} + \tilde{f}(\eta; p) \frac{\partial^2 \tilde{f}(\eta; p)}{\partial \eta^2} - 2 \left(\frac{\partial \tilde{f}(\eta; p)}{\partial \eta} \right)^2, \quad (3.27)$$

$$\begin{aligned} \mathcal{N}_\theta [\tilde{\theta}(\eta; p), \tilde{\phi}(\eta; p), \tilde{f}(\eta; p)] &= \frac{1}{\text{Pr}} \left(1 + \frac{4}{3} R \right) \frac{\partial^2 \tilde{\theta}(\eta; p)}{\partial \eta^2} + Nt \left(\frac{\partial \tilde{\theta}(\eta; p)}{\partial \eta} \right)^2 + \tilde{f}(\eta; p) \frac{\partial \tilde{\theta}(\eta; p)}{\partial \eta} \\ &+ Nb \left(\frac{\partial \tilde{\theta}(\eta; p)}{\partial \eta} \frac{\partial \tilde{\phi}(\eta; p)}{\partial \eta} \right) - \tilde{\theta}(\eta; p) \frac{\partial \tilde{f}(\eta; p)}{\partial \eta} \end{aligned} \quad (3.28)$$

$$- St \left(\frac{\partial \tilde{f}(\eta; p)}{\partial \eta} \right) + Ec \left(\frac{\partial^2 \tilde{f}(\eta; p)}{\partial \eta^2} \right)^2, \quad (3.29)$$

$$\begin{aligned} \mathcal{N}_\phi [\tilde{\phi}(\eta; p), \tilde{f}(\eta; p), \tilde{\theta}(\eta; p)] &= \frac{\partial^2 \tilde{\phi}(\eta; p)}{\partial \eta^2} + \frac{Nt}{Nb} \left(\frac{\partial^2 \tilde{\theta}(\eta; p)}{\partial \eta^2} \right) - ScSm \left(\frac{\partial \tilde{f}(\eta; p)}{\partial \eta} \right) \\ &+ Sc \left(\tilde{f}(\eta; p) \frac{\partial \tilde{\phi}(\eta; p)}{\partial \eta} - \tilde{\phi}(\eta; p) \frac{\partial \tilde{f}(\eta; p)}{\partial \eta} \right). \end{aligned} \quad (3.30)$$

As p grows up from 0 to 1, initial guesses $f_0(\eta)$, $\theta_0(\eta)$ and $\phi_0(\eta)$ progressively approaches to the final solution $f(\eta)$, $\theta(\eta)$ and $\phi(\eta)$. For $p = 0$ and $p = 1$, one respectively has

$$\tilde{f}(\eta; 0) = f_0(\eta), \quad \tilde{f}(\eta; 1) = f(\eta), \quad (3.31)$$

$$\tilde{\theta}(\eta; 0) = \theta_0(\eta), \quad \tilde{\theta}(\eta; 1) = \theta(\eta), \quad (3.32)$$

$$\tilde{\phi}(\eta; 0) = \phi_0(\eta), \quad \tilde{\phi}(\eta; 1) = \phi(\eta). \quad (3.33)$$



Expanding $\tilde{f}(\eta; p)$, $\tilde{\theta}(\eta; p)$ and $\tilde{\phi}(\eta; p)$ in accordance with the Power series we have:

$$\begin{aligned}\tilde{f}(\eta; p) &= f_0(\eta) + \sum_{m=1}^{\infty} f_m(\eta) p^m, \quad f_m(\eta) = \frac{1}{m!} \left. \frac{\partial^m \tilde{f}(\eta; p)}{\partial p^m} \right|_{p=0}, \\ \tilde{\theta}(\eta; p) &= \theta_0(\eta) + \sum_{m=1}^{\infty} \theta_m(\eta) p^m, \quad \theta_m(\eta) = \frac{1}{m!} \left. \frac{\partial^m \tilde{\theta}(\eta; p)}{\partial p^m} \right|_{p=0}, \\ \tilde{\phi}(\eta; p) &= \phi_0(\eta) + \sum_{m=1}^{\infty} \phi_m(\eta) p^m, \quad \phi_m(\eta) = \frac{1}{m!} \left. \frac{\partial^m \tilde{\phi}(\eta; p)}{\partial p^m} \right|_{p=0},\end{aligned}\tag{3.34}$$

where the convergence depends upon \hbar_f , \hbar_θ and \hbar_ϕ . Assume that \hbar_f , \hbar_θ and \hbar_ϕ are chosen such that the series (3.34) converges at $p = 1$ thus

$$\begin{aligned}f(\eta) &= f_0(\eta) + \sum_{m=1}^{\infty} f_m(\eta), \\ \theta(\eta) &= \theta_0(\eta) + \sum_{m=1}^{\infty} \theta_m(\eta), \\ \phi(\eta) &= \phi_0(\eta) + \sum_{m=1}^{\infty} \phi_m(\eta).\end{aligned}\tag{3.35}$$

3.2.2 mth-order deformation problems

By taking the differentiation m times of the given equations Eqs. (3.21) – (3.26), with respect to p then dividing by $m!$ we get

$$\mathcal{L}_f [f_m(\eta) - \chi_m f_{m-1}(\eta)] = \hbar_f \mathcal{R}_m^f(\eta),\tag{3.36}$$

$$f_m(0) = f'_m(0) = f'_m(\infty) = 0,\tag{3.37}$$

$$\mathcal{L}_\theta [\theta_m(\eta) - \chi_m \theta_{m-1}(\eta)] = \hbar_\theta \mathcal{R}_m^\theta(\eta),\tag{3.38}$$

$$\theta_m(0) = \theta_m(\infty) = 0,\tag{3.39}$$

$$\mathcal{L}_\phi [\phi_m(\eta) - \chi_m \phi_{m-1}(\eta)] = \hbar_\phi \mathcal{R}_m^\phi(\eta),\tag{3.40}$$

$$\phi_m(0) = \phi_m(\infty) = 0,\tag{3.41}$$

in which

$$\mathcal{R}_m^f(\eta) = \left[f_{m-1}''' + \sum_{k=0}^{m-1} [f_{m-1-k} f_k'' - 2f_{m-1-k}' f_k'] - (M + \lambda) f_{m-1}' \right], \quad (3.42)$$

$$\begin{aligned} \mathcal{R}_m^\theta(\eta) = & \frac{1}{\text{Pr}} \left(1 + \frac{4}{3} R \right) \theta_{m-1}'' + Nt \sum_{k=0}^{m-1} \theta_{m-1-k}' \theta_k' + Nb \sum_{k=0}^{m-1} \phi_{m-1-k}' \theta_k' \\ & + \text{Ec} \sum_{k=0}^{m-1} f_{m-1-k}'' f_k'' - \sum_{k=0}^{m-1} f_{m-1-k}' \theta_k + \sum_{k=0}^{m-1} \theta_{m-1-k}' f_k - St (f_{m-1}') , \end{aligned} \quad (3.43)$$

$$\mathcal{R}_m^\phi(\eta) = \phi_{m-1}'' + \left(\frac{Nt}{Nb} \right) \theta_{m-1}'' - Sc Sm f_{m-1}' + Sc \sum_{k=0}^{m-1} [f_{m-1-k} \phi_k' - \phi_{m-1-k} f_k'] , \quad (3.44)$$

$$\chi_m = \begin{cases} 0, & m \leq 1, \\ 1, & m > 1, \end{cases} \quad (3.45)$$

and the general solutions are

$$f_m(\eta) = f_m^*(\eta) + D_1 + D_2 e^\eta + D_3 e^{-\eta}, \quad (3.46)$$

$$\theta_m(\eta) = \theta_m^*(\eta) + D_4 e^\eta + D_5 e^{-\eta}, \quad (3.47)$$

$$\phi_m(\eta) = \phi_m^*(\eta) + D_6 e^\eta + D_7 e^{-\eta}, \quad (3.48)$$

where f_m^* , θ_m^* and ϕ_m^* are the special solutions.

3.3 Convergence of HAM solution

Homotopy analysis method (HAM) involves embedding parameter \hbar which play a vital role to control the convergence of the series solution. The suitable range for admissible values of \hbar can be evaluated by sketching the \hbar -curves for velocity, temperature and concentration profiles. The admissible values of \hbar_f , \hbar_θ and \hbar_ϕ are $-1 \leq \hbar_f \leq -0.2$, $-0.95 \leq \hbar_\theta \leq -0.3$ and $-0.9 \leq \hbar_\phi \leq -0.35$ as shown in Figure (3.2). It is important to note that the series solution is convergent for whole range of η ($0 < \eta < \infty$) when $\hbar_f = \hbar_\theta = \hbar_\phi = -0.8$.

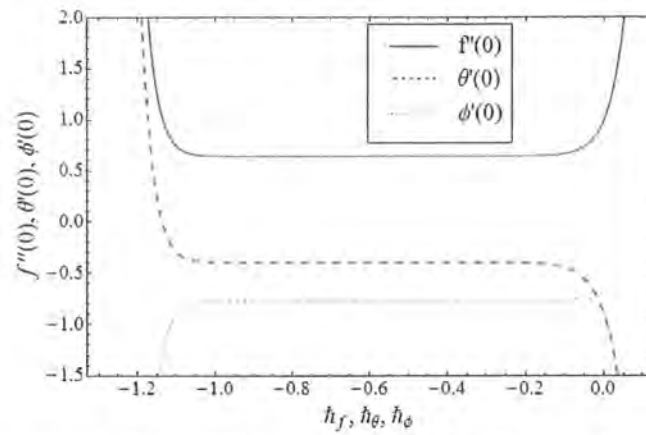


Figure 3.2: Combined h -curves for $f''(0)$, $\theta'(0)$ and $\phi'(0)$.

Table 3.1. HAM series solutions converge at different order of approximations when $Pr = 1.7$, $Sc = 1.1$, $\lambda = Sm = St = M = 0.1$, $Ec = 0.5$, $Nt = Nb = 0.8$ and $R = 0.4$.

Order of approximations	$-f''(0)$	$-\theta'(0)$	$-\phi'(0)$
1	1.3467	0.49636	0.62000
10	1.3589	0.39716	0.78108
20	1.3590	0.39758	0.77459
25	1.3590	0.39761	0.77414
33	1.3590	0.39762	0.77406
37	1.3590	0.39762	0.77404
40	1.3590	0.39762	0.77404
45	1.3590	0.39762	0.77404
50	1.3590	0.39762	0.77404
45	1.3590	0.39762	0.77404
50	1.3590	0.39762	0.77404
55	1.3590	0.39762	0.77404



3.4 Graphical results and discussion

The analytical solutions are obtained for velocity $f'(\eta)$, temperature $\theta(\eta)$ and concentration fields $\phi(\eta)$ for various values of pertinent parameters. Obtained results are displayed through graphs. The effect of Hartman number M on the velocity field $f'(\eta)$ is shown in Figure (3.3). This figure reveals that the increasing values of M results in a decrease in the velocity profile. This is due to the fact that an increment in M , enhances the effect of magnetic damping force, called a Lorentz force, which has the tendency to retard the fluid motion. Thus the resistance offered by Lorentz force to the flow yields a reduction in the fluid velocity. It is clearly shown in Figure (3.4) that the larger values of porosity parameter λ leads to a reduction in velocity field $f'(\eta)$. This is evident from the fact that the porosity parameter depends on the permeability parameter K (see Eq. (3.15)). This lower permeability parameter K corresponds to larger values of the porosity parameter λ and hence the reduction in the fluid velocity is inquired.

The variation in temperature profile $\theta(\eta)$ under the influence of Brownian motion parameter Nb and thermophoresis parameter Nt is captured in Figures (3.5) and (3.6) respectively. From the Figure (3.5) we have noticed that an increase in Nb results in an increase in the temperature profile. This is due to the fact that Brownian motion is actually for random motion of nanoparticles in base fluid. So, with increasing values of Nb nanoparticles vibrate haphazardly and temperature profile increases. The variation of thermophoresis parameter Nt on temperature profile is depicted in Figure (3.6). It reveals that the temperature profile and thermal boundary layer thickness increases when thermophoresis parameter Nt increases. Increase in thermal stratified parameter St yields a reduction in the temperature difference between surface and ambient fluid as illustrated in Figure (3.7). Figure (3.8) demonstrates the decreasing behavior of the temperature profile with the increase in Prandtl number Pr . This is quite in accordance with the fact that the ratio of momentum diffusivity to thermal diffusivity is signified as the Prandtl number Pr . Thermal diffusivity decreases by increasing Pr and heat diffuses away slowly from the heated surface and thus temperature decreases. The temperature profile for different values of R is plotted in Figure (3.9). It has been noticed from the figure that temperature increases and its corresponding boundary layer gets thicker for larger values of R . On increasing the values of Ec number, temperature of the fluid also increases. The variation in temperature predict that the viscosity of the fluid is sensitive in nature. Due to the fact of the

drag forces, Eckert number Ec stores heat energy within the fluid thus the temperature profile increases (see Figure (3.10)).

Effect of different parameters on concentration profile are depicted in Figure (3.11 – 3.14). Figure (3.11) portrays that by increasing Sc , the concentration profile decreases. An increment in the solutal stratification parameter Sm yields a decrease in concentration profile as demonstrated in Figure (3.12). Figure (3.13) shows the variation of concentration profile corresponding to the larger values of Brownian motion parameter Nb . Here concentration profile decreases via Nb . Figure (3.14) discloses that the concentration profile increases with the increase in Nt .

Table (3.1) is tabulated to show the convergence of the series solutions for velocity, temperature and concentration profiles. Analysis of Table (3.1) reveals that the convergence is achieved at 20, 33 and 37th orders of approximations respectively. Numerical values of skin friction coefficient for different values of Hartman number M and porosity parameter λ are given in Table (3.2). We observed that increasing values of M and λ yield a increase in skin friction coefficient. Variation in local Nusselt number Nu (heat transfer coefficient) and Sherwood number Sh (mass transfer coefficient) for different values of Sc , Nb , Nt , St and Sm is shown in Table (3.3) with the fixed values of other parameters as $\lambda = 0.1$, $Pr = 1.7$, $R = 0.4$, $M = 0.1$ and $Ec = 0.5$. Here we noticed that increasing values of Sm and St exhibit the enhancement in both Nusselt and Sherwood numbers, whereas Nusselt and Sherwood numbers decreases for larger Nt . For Nb and Sc Nusselt and Sherwood numbers portrays an opposite behavior.

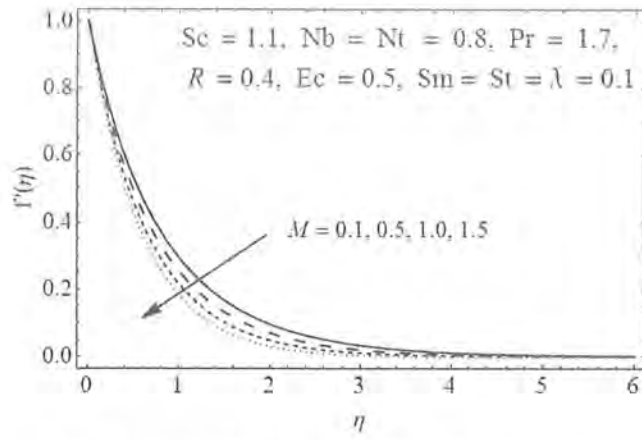


Figure 3.3: Impact of M on velocity $f'(\eta)$

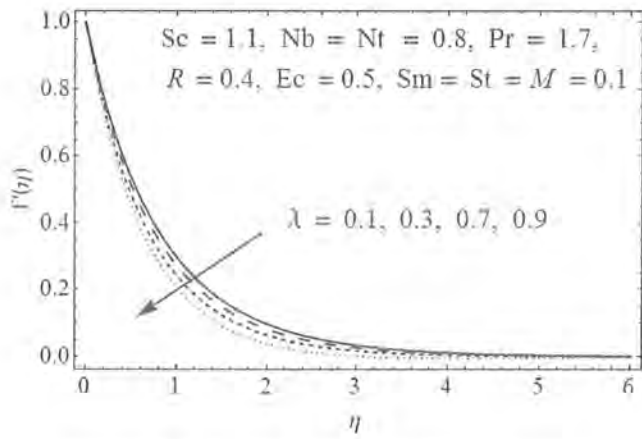


Figure 3.4: Impact of λ on velocity $f'(\eta)$

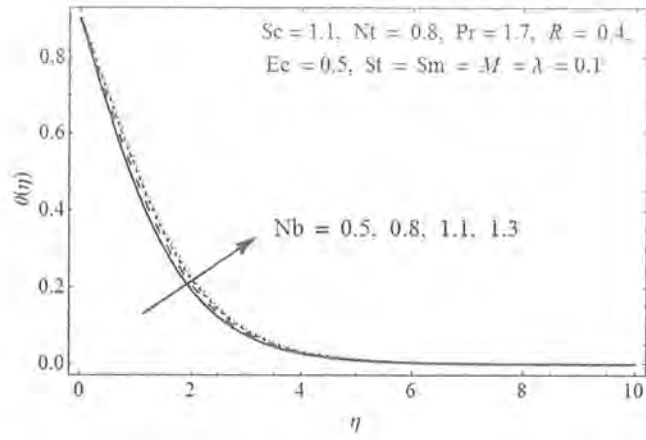


Figure 3.5: Impact of Nb on temperature $\theta(\eta)$.

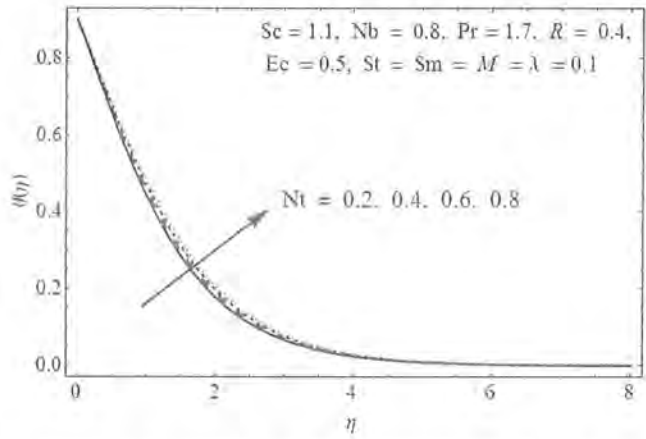


Figure 3.6: Impact of Nt on temperature $\theta(\eta)$.

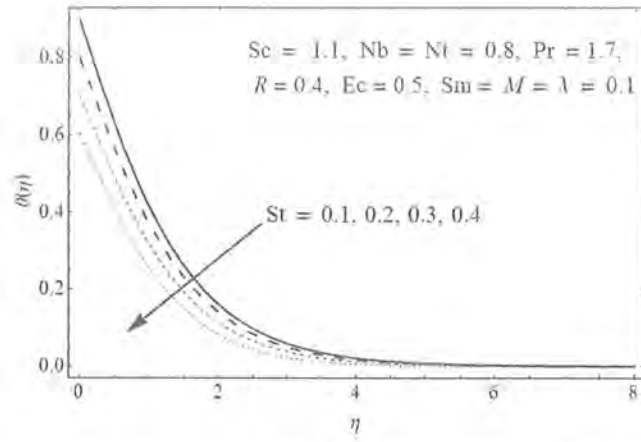


Figure 3.7: Impact of St on temperature $\theta(\eta)$.

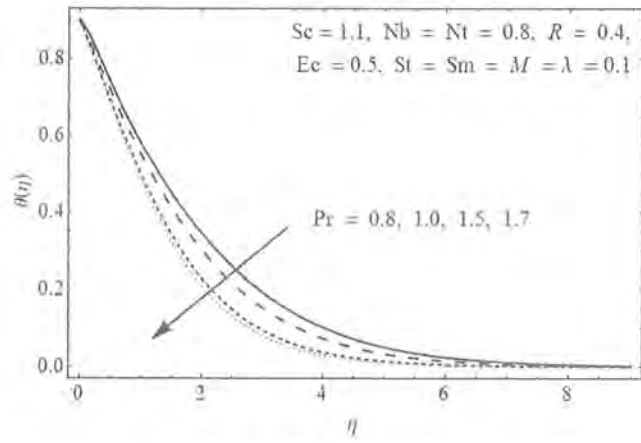


Figure 3.8: Impact of Pr on temperature $\theta(\eta)$.

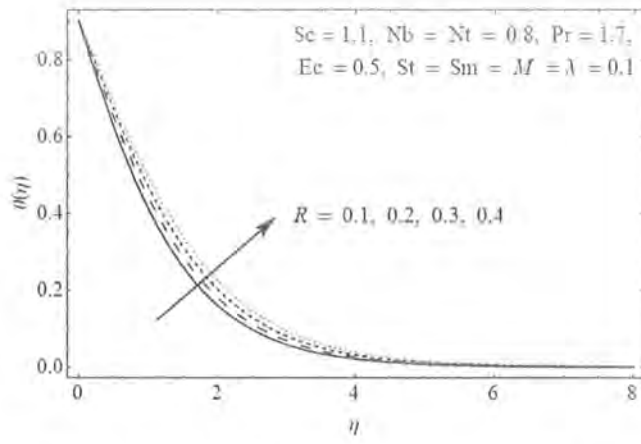


Figure 3.9: Impact of R on temperature $\theta(\eta)$.

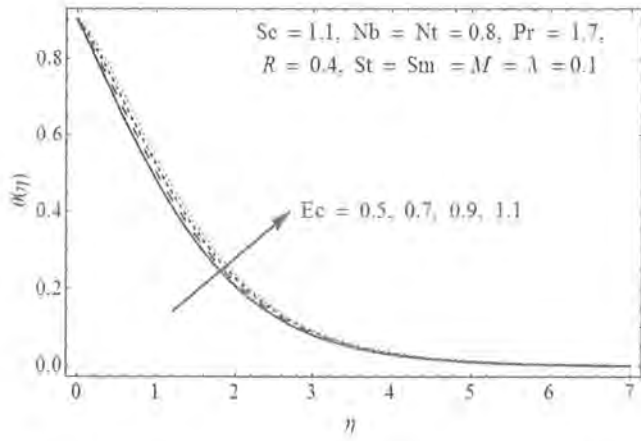


Figure 3.10: Impact of Ec on temperature $\theta(\eta)$.

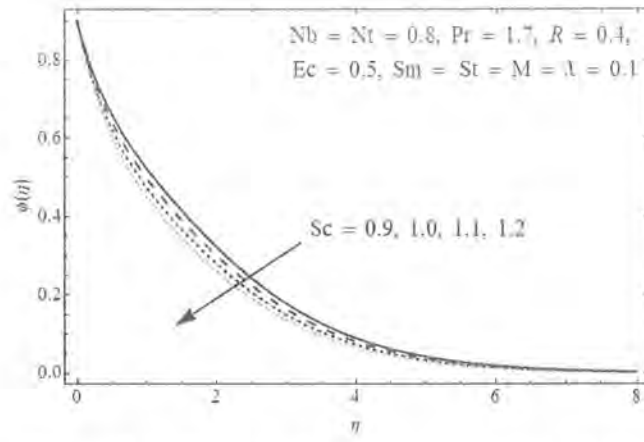


Figure 3.11: Impact of Sc on concentration $\theta(\eta)$.

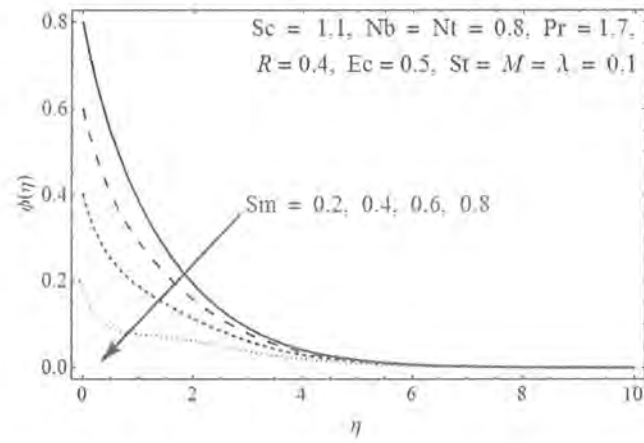


Figure 3.12: Impact of Sm on concentration $\phi(\eta)$.

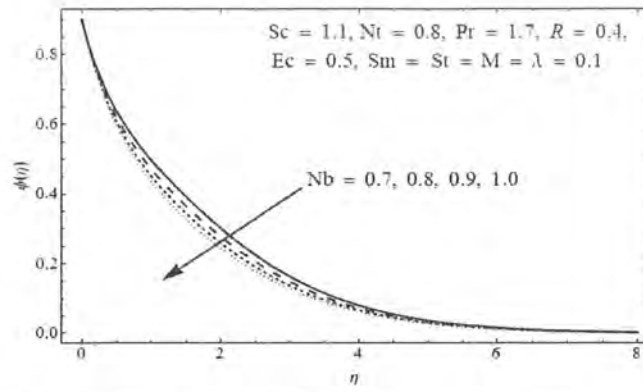


Figure 3.13: Impact of Nb on concentration $\phi(\eta)$.

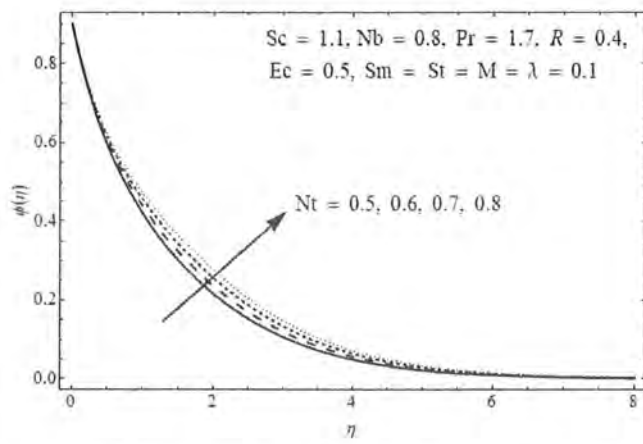


Figure 3.14: Impact of Nt on concentration $\phi(\eta)$.



Table 3.2: Numerical values skin friction coefficient when $Pr = 1.7$, $Sc = 1.1$, $\lambda = Sm = St = M = 0.1$, $Ec = 0.5$, $Nt = Nb = 0.8$ and $R = 0.4$.

M	λ	$-f''(0)$
0.1	0.1	1.3590
0.2		1.3958
0.3		1.4316
0.5		1.4665
	0.3	1.3958
	0.4	1.4316
	0.5	1.4665

Table 3.3: Numerical values of Nusselt and Sherwood numbers when $Pr = 1.7$, $Sc = 1.1$, $\lambda = Sm = St = M = 0.1$, $Ec = 0.5$, $Nt = Nb = 0.8$ and $R = 0.4$

Sm	St	Nb	Nt	Sc	$(1 + \frac{4R}{3}) \left(\frac{-1}{1-St} \right) \theta'(0)$	$\left(\frac{-1}{1-Sm} \right) \phi'(0)$
0.1	0.1	0.8	0.8	1.1	0.6774	0.9381
0.2					0.6940	0.9979
0.4					0.7285	1.0668
0.5					0.7463	1.1904
	0.2				0.7374	0.8609
	0.3				0.8130	0.8622
	0.4				0.9117	0.8638
		0.6			0.7419	0.7498
		0.7			0.7089	0.8132
		0.9			0.6472	0.8957
			0.6		0.7053	0.9020
			0.7		0.6911	0.8804
			0.9		0.6442	0.8407
				1.0	0.6911	0.7774
				1.2	0.6651	0.9381
				1.3	0.6541	1.0122

3.5 Key findings

This chapter contained an analytical solution of MHD boundary layer nanofluid flow beyond a exponential stretched surface having the thermal radiation, porous and double stratified medium. By taking the larger values of Hartman number M and porosity parameter λ a decreasing behavior of the velocity profile $f(\eta)$ is examined. For higher values of Nb and Nt parameters, the temperature profile enhances. Temperature profile decreases with an increment in St . The effect of Prandtl number Pr is to reduce the temperature and thermal boundary layer thickness. Radiation effect enhances the thermal stratified fluid and exhibits the same behavior. It is worth mentioning that the temperature and its associated boundary layer thickness is a

increasing function of Ec . Concentration profile decreases for increasing values of Sm . Nb and Nt parameter exhibits an opposite behavior in concentration profile. Skin friction coefficient increases for both M and λ . The dimensionless local Nusselt number increases with an increase in Pr . The local Nusselt number increases for higher values of Sm and St while it decreases for larger Sc , Nb and Nt . Local Sherwood number enhances by increasing Sm , St , Sc and Nb .



Bibliography

- [1] S. U. S. Choi, Enhancing thermal conductivity of fluids with nanoparticles, *ASME Int. Mech. Eng.* 66 (1995) 99 – 105.
- [2] J. Buongiorno, Convective transport in nanofluids, *J. Heat Transf.* 128 (2005) 240 – 250.
- [3] M. Turkyilmazoglu, Unsteady convection flow of some nanofluids past a moving vertical flat plate with heat transfer, *J. Heat Transf.* 136 (3) (2013) 031704.
- [4] M. Turkyilmazoglu, Nanofluid flow and heat transfer due to a rotating disk, *Computers & Fluids* 94 (2014) 139 – 146.
- [5] M. Sheikholeslami and M. Gorji-Bandpy, Free convection of ferrofluid in a cavity heated from below in the presence of an external magnetic field, *Powder Technology* 256 (2014) 490 – 498.
- [6] M. Sheikholeslami, M. Gorji-Bandpy and D. D. Ganji, Lattice Boltzmann method for MHD natural convection heat transfer using nanofluid, *Powder Technology* 254 (2014) 82 – 93.
- [7] T. Hussain, S. A. Shehzad, T. Hayat, A. Alsaedi, F. Al-Solamy and M. Ramzan, Radiative hydromagnetic flow of Jeffrey nanofluid by an exponentially stretching sheet, *Plos One* 9 (8) (2014) e103719.
- [8] M. M. Rashidi, S. Abelman and N. F. Mehr, Entropy generation in steady MHD flow due to a rotating porous disk in a nanofluid, *Int. J. Heat Mass Transf.* 62 (2013) 515 – 525.
- [9] J. Niu, C. Fu and W. C. Tan, Slip flow and heat transfer of a non-Newtonian nanofluid in a microtube, *Plos One* 7 (5) (2012) e37274.



- [10] S. Khalili, S. Dinarvand, R. Hosseini, H. Tamim and I. Pop, Unsteady MHD flow and heat transfer near stagnation point over a stretching/shrinking sheet in porous medium filled with a nanofluid, *Chin. Phy. B* 23 (4) (2014) 048203.
- [11] M. Sheikholeslami, R. Ellahi, H.R. Ashorynejad, G. Domairry and T. Hayat, Effects of heat transfer in flow of nanofluids over a permeable stretching wall in a porous medium, *J. Comp. Theo. Nanosci.* 11 (2014) 486 – 496.
- [12] I. Pop, A note on MHD flow over a stretching permeable surface, *Mech. Res. Comm.* 25 (1998) 263 – 369.
- [13] L. J. Crane, Flow past a stretching plate, *J. Appl. Math. Phy. (ZAMP)* 21 (1970) 645 – 647.
- [14] S. Mukhopadhyay, Slip effects on MHD boundary layer flow over an exponentially stretching sheet with suction/blowing and thermal radiation, *Ain Shams Eng. J.* 4 (2013) 485–491.
- [15] M. Turkyilmazoglu, Exact solutions for two-dimensional laminar flow over a continuously stretching or shrinking sheet in an electrically conducting quiescent couple stress fluid, *Int. J. Heat Mass Transf.* 72 (2014) 1 – 8.
- [16] W. Ibrahim, B. Shankar and M. M. Nandeppanavar, MHD stagnation point flow and heat transfer due to nanofluid towards a stretching sheet, *Int. J. Heat Mass Transf.* 56 (2013) 1 – 9.
- [17] A. Malvandi, F. Hedayati and D. D. Ganji, Slip effects on unsteady stagnation point flow of a nanofluid over a stretching sheet, *Powder Technology* 253 (2014) 377 – 384.
- [18] T. Hayat, M. Imtiaz, A. Alsaedi and R. Mansoor, MHD flow of nanofluids over an exponentially stretching sheet in a porous medium with convective boundary conditions, *Chin. Phy. B* 23 (5) (2014) 054701.
- [19] W. Ibrahim, and O. D. Makinde, The effect of double stratification on boundary layer flow and heat transfer of nanofluid over a vertical plat, *Computer & Fluids* 86 (2013) 433 – 441.
- [20] S. Mukhopadhyay, MHD boundary layer flow and heat transfer over an exponentially stretching sheet embedded in a thermally stratified medium, *Alex. Eng. J.* 52 (2013) 259 – 265.

- [21] D. Srinivasacharya and M. Uppendar, Effect of double stratification on MHD free convection in a micropolar fluid. *J. Egypt. Math. Soc.* 21 (2013) 370 – 378.
- [22] T. Hayat, S. A. Shehzad, H. H. Al-Sulami and S. Asghar, Influence of thermal stratification on the radiative flow of Maxwell fluid, *J. Braz. Soc. Mech. Sci. Eng.* 35 (2013) 381 – 389.
- [23] T. Hayat, Z. Hussain, M. Farooq, A. Alsaedi and M. Obaid, Thermally stratified stagnation point flow of an Oldroyd-B fluid. *Int. J. Nonlinear Sci. Numer. Simulat.* 15 (2014) 77 – 86.
- [24] M. Hassani, M. M. Tabar, H. Nemati, G. Domairry and F. Noori, An analytical solution for boundary layer flow of a nanofluid past a stretching sheet, *Int. J. Therm. Sci.* 11 (2011) 2256 – 2263.
- [25] S. J. Liao, *Beyond Perturbation: Introduction to Homotopy Analysis Method*, Chapman and Hall/CRC Press, Boca Raton (2003).
- [26] S. Abbasbandy, R. Naz, T. Hayat and A. Alsaedi, Numerical and analytical solutions for Falkner–Skan flow of MHD Maxwell fluid, *Appl. Math. Comp.* 242 (2014) 569 – 575.
- [27] U. Farooq, T. Hayat, A. Alsaedi and S. J. Liao, Heat and mass transfer of two-layer flows of third-grade nanofluids in a vertical channel, *Appl. Math. Comp.* 242 (2014) 528 – 540.
- [28] M. M. Rashidi, M. Ali, N. Freidoonimehr, B. Rostami and A. Hossian, Mixed convection heat transfer for viscoelastic fluid flow over a porous wedge with thermal radiation, *Adva. Mech. Eng.* 204 (2014) 735939.
- [29] S. A. Shehzad, A. Alsaedi, T. Hayat and M. S. Alhuthali, Thermophoresis particle deposition in mixed convection three-dimensional radiative flow of an Oldroyd-B fluid, *J. Taiwan Inst. Chem. Eng.* 45 (2014) 787 – 794.
- [30] M. Mustafa, M. A. Farooq, T. Hayat and A. Alsaedi, Numerical and series solutions for stagnation point flow of nanofluid over an exponentially stretching sheet, *Plos One* 8 (5) (2013) e61859.

